



CHAPTER V

POLYTHIOPHENE COATED LATEX PARTICALS BY ADMICELLAR POLYMERIZATION

5.1 Abstract

Conducting polymers (CPs) were first produced in the mid-1970s as a novel generation of organic materials that have both electrical and optical properties similar to those of metals and inorganic semiconductors, but which also exhibit the attractive properties associated with conventional polymers, such as ease of synthesis and flexibility in processing. Polythiophene (PTh) is one of the interesting conductive polymers. In an aqueous or organic medium, PTh can be blended with an insulating polymer, eg. rubber, to produce conducting polymer composites with good conductivity and superior mechanical properties. To overcome these limitations, electrochemical and admicellar polymerization with Sodium Dodecyl Sulfate (SDS) is used. The admicellar polymerization of PTh by electrochemical method over natural rubber particles was investigated by varying monomer content and applied voltages. The success of synthesis was confirmed by FTIR, SEM, and TEM. The TGA curves of the admicelled products revealed a shift to higher decomposition temperature than that of pure PTh. The mechanical properties of the admicelled rubber were also developed to be stiffer than that of natural rubber. The conductivity of the modified rubber is about 10^{-12} to 10^{-6} S/cm, which is much higher than that of natural rubber by several orders. Conductive rubbers can be used instead of metallic conductors because the soft materials have obvious advantages of flexibility and ability to absorb mechanical shock.

Key-words: Polythiophene, conductive polymer, admicelle technique, electrochemical polymerization, natural rubber modification, morphology of PTh.

5.2 Introduction

The synthesis of conducting polymers has attracted great attention owing to their possible application as electronic materials, gas sensors, electromagnetic shielding coatings, etc. Several studies on the preparation of conducting polymer-like polypyrrole, polythiophene, and their derivatives revealed that these materials are electrically conductive, though they are poor in mechanical properties.^[85] Homogeneous composites using an insulating polymer matrix became one of the major solutions for the invention of conducting polymer with better physical and mechanical properties.^{[122][123]} Furthermore, some studies revealed that there might exist a chemical interaction between the thiophene oligomer and the insulating polymers during the electrochemical synthesis.^[124]

The major feature of conductive organic polymers such as polythiophene(PT) is that all contain a π electron structure extending throughout their configuration. These polymers generally are insulators or semiconductors but can be made as conductive as metals when they are subjected to a doping process. It is highly conductive in an oxidized state. The conductance process in these polymers is believed to take place by electron "delocalization".^[125-126]

Organic polymers have very complicated morphological structures, depending on the method of synthesis. Therefore, their properties vary according to their structure features. It is very difficult to obtain the same material if the synthesis conditions are changed.

Whiffen et al.(1979)^[125] proposed a two-step mechanism for the polymerization of thiophene monomers. As shown in Figure 5.1, polymerization starts with the formation of a cation radical that is formed by a loss of an electron from the monomer. Thiophene radical can either give a substitution or combination reaction. The oxidation of thiophene is irreversible. The cation radical can be formed in the first step as depicted in Figure 5.1. Thiophene is extremely reactive.

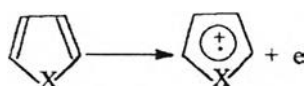


Figure 5.1 Oxidation of conductive polymer; X represents a hetero atom as nitrogen (for Polypyrrole) or sulfur (for Polythiophene).

Recently, our group research reported the success of polypyrrole (PPy) coated on the surface of natural rubber particles by admicellar polymerization using the Dodecyl Sulfate Sodium salt (SDS) as surfactant at various pyrrole concentrations [Bussomsit, K.2002]. In this study, natural rubber particles use as the substrates for electrochemical admicelled polymerization of polythiophene using SDS as the as the surfactant. This research focuses on the influences of thiophene content and thiophene content, pH, reaction times, and voltage on the morphology. Furthermore, the mechanical properties, thermal properties, and conductivity were investigated.

5.3 Experimental

5.3.1 Materials

In this research, the natural rubber latex used as the substrate for electrochemical polymerization was provided by Rubber Research Institute, ~60% DRC. The anionic surfactant, selected for this experiment was Sodium Dodecyl Sulfate (SDS). A schematic of the chemical structure of SDS is shown in Figure 3.1. SDS was purchased from Aldrich Chemical Company, Ltd. with 99% purity^[89]. According to Rosen (1996) the CMC of SDS was determined to be $\sim 1.58 \times 10^{-3} \text{ mol/dm}^3$ at 25 °C. Hydrochloric acid used as doping and adjust PH. The thiophene monomer (Fluka) was first purified by distillation, and thereafter stored refrigerated at 4 °C before use in the polymerization. Thiophene monomer: purum 98% GC, Mr= 84.14, bp=82-84 °C, $d_4^{20}=1.063$ contains 0.2% benzene.

5.3.2 Equipments

The instruments and ASTMs are shown in Table 5.1 and 5.2, respectively.

Table 5.1 Parameters to be measured for admicelled rubber properties

Parameters	Instrument / Technique
Prepared and purified natural rubber	-Hot plate and magnetic stirrer -Centrifugator, Hermle Z383K (at 10000 rpm/20 min) (ASTM 1076-02)
Particle Size	-Particle Size Analyzer (Mastersizer X Ver 2.15) (45 mm)

	lens, active beam length 2.4 mm)
Thermal properties and amount of polymer formed	Thermogravimetric Analyzer (Perkin Elmer, Pyris Diamond) Thailand co.,ltd
Surface morphology	Scanning electron microscope (SEM) (JEOL JSM-5200) with magnification range between 1000-5000 times using voltage 15 kv
Atomic morphology	Transmission electron microscope (TEM) (JEOL JEM-2100)
Tensile testing	-Lloyd LRX Universal Testing Machine (ASTM D882-91) -Instron Universal Testing Machine under (ASTM638M-91a)
Functional group	Fourier Transform Infrared Spectroscopy (FTIR) (Nexus 670, HATR flat plate system with 45°C ZnSe crystal) PERKIN ELMER 1760X.
Surface and volume conductivity	Resistivity Test Fixture (Keithley Model 8009) and Electrometer/High Resistance Meter (Keithley 6517A). (ASTM D257-99)
Density	Sartorius approach, model :YDK01

Table 5.2 Test method and ASTM

Property	method	Instrument
Tensile properties (Max stress, MPa Elongation to break, % modulus, MPa)	ASTM 638M-91a ASTM D882-91	Instron Model 1011 Lloyd Instruments LS 500
Hardness, Shore A and Shore D	ASTM D2240	Lever Loader Model 716
Tear strength	ASTM D2262-83	Lloyd Instruments LS 500

5.3.3 Purification of the Natural Rubber Latex

The rubber latex has a 60%wt dried solid content. Rubber latex (4-8 g) was mixed with 50 ml distilled water and centrifuged two times at 20°C, 10000 rpm for

20 minutes to removed dissolved impurities. Then, particles were resuspended in water and adjust pH <3.0 by using HCl.

5.3.4 Particle Size Measurement

The particle size of natural rubber was determined by a particle size analyzer, Masterizer X version 2.15 (Malvern Instruments Ltd.). The lens used in this experiment was 45 mm for particle size 0.1-80 μm and active beam length was set at 24 nm. The sample was placed in a sample cell across a laser beam. This machine analyzed the average particle size and standard size distribution from the laser beam depending on the beam length parameter. Consequently, the specific surface area was calculated from the particle diameter with the assumption of constant volume of a spherical particle.

A droplet of surfactant was added in a stirring water chamber in order to aid the distribution of natural rubber in water. After that, 0.03 vol% of natural rubber aqueous solution was suspended in a stirring water chamber.

5.3.5 Polymerization of Thiophene onto Latex Particles

A.) Prepared Admicellar Polymerization of Pyrrole onto Latex Particles

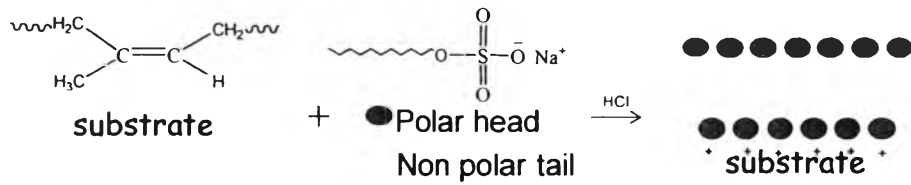
Concentrated natural rubber latex (4-8 g) was mixed with 50 ml distilled water and centrifuged two times at 20°C, 10000 rpm for 20 minutes. The 25 g of cream was separated and added in 10 ml distilled water. Then the rubber latex was mixed with surfactant solution, SDS, 16 mM, and make up volume to 500 ml (including amount of Thiophene at various concentration 20-800 mM, 0.79-31.66 ml) by distilled water. HCl was added to maintain the pH of the solution at 3.0, which is the pH below the point of zero charge [11]. Then, it is stirred four hours to let the surfactant molecules form the bilayer at the surface of the rubber particles (Figure 5.2a).

The thiophene solution (20–800 mM, 0.79–31.66 ml) was added and left for 1 hour (Figure 5.2b). Next, the apparatus for electrolysis was set up, and the aqueous solution was poured into the reaction bottle. Then, an additional current was passed though the solution containing the pyrrole monomer at various voltages and the solution was purge with N_2 to prevent the oxidation in the system (Figure 5.2c). As the current was applied across the cell, pyrrole was polymerized in the rubber latex solution at the cathode. The rubber was also pulled to cathode during polymerization and

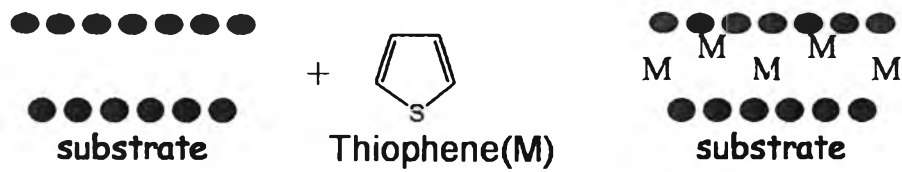
finally conductive natural rubber occurred on the cathode, (the copper has a dimension of 3.5x7 cm), as shown in Figure 5.3.

After the electro-polymerization has started, the pH and mass on the electrode are checked every hour and the electrode was replaced. The pH was adjusted to 3.0 by HCl. After the polymerization was complete, the dark solid rubber on the working electrode was washed with water to remove the surfactant, followed by drying in a vacuum oven at 70°C for 12 hours and black sheet with a constant weight was obtained. The solution changed from white to black and finally to clear solution (Figure 5.2d). In order to obtain the best synthesized conditions, factors such as applied potential (voltage), time, %yield and pH were studied. Mass can also be controlled by these factors. The voltage was applied by using an adaptor (0-30 Voltage, 3A, Kenji-model: K01). The average electrode sizes were about 3.5 x 7cm.

a. Step 1. Admicelle Formation



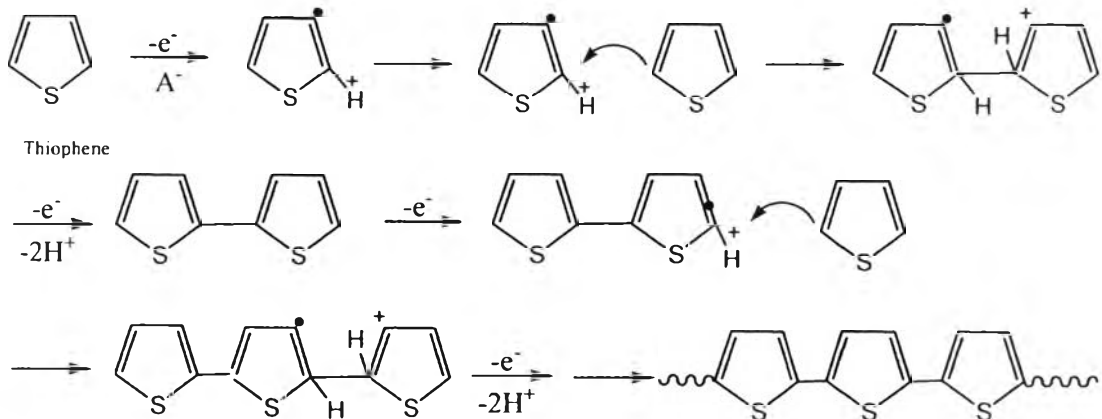
b. Step 2. Monomer Adsorption



c. Step 3. Polymer formation



Applied voltage



d. Step 4. Surfactant Removal

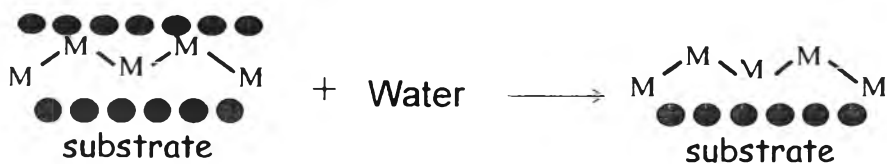


Figure 5.2 phenomena of admicelled polymerization

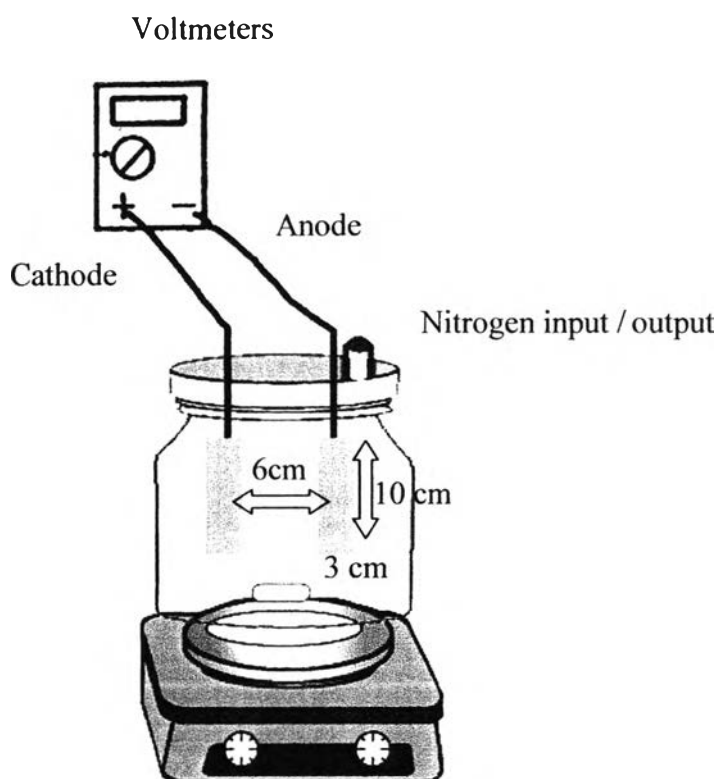


Figure 5.3 Apparatus for admicelled polymerization with electrolysis. It consists of a reaction bottle and cover, cathode and anode electrodes, a voltmeter, an ammeter, a current supply, a hot plate and a magnetic stirrer.

5.3.6 FT-IR Observation

The adsorption of the admicelled rubber films with a thickness of 0.3–0.8 mm obtained by compression at 160°C under a pressure of 25 tons for 15 min, were determined using the horizontal attenuated total reflection accessories for the FTIR (Nexus 670, HATR module) to measure the spectra of materials. The spectra were recorded in the absorbance mode in a wavenumber range of 400–4000 cm^{-1} . The sample spectra were recorded by using air as a background.

The KBr technique was used to prepare the powder sample of pure PPy for recording the spectrum. The specimen of pure PPy was prepared by grinding the powdered PPy with the KBr powder. The mixture was molded in special dies under a pressure of 10 tons. The sample spectrum was recorded by using KBr as a background.

5.3.7 Determination density

The density of the specimens was measured using the Sartorius approach, model:YDK01, where the sample is weighed in air and then in water by a balance with a reproducibility better than 10 μg . Each measurement represented the average of at least 3 specimens.

Density of H₂O 0.9964 (from table at 25°C)
temperature 27.5

$$\text{Eq} \quad d = \frac{w_a \times d_{H_2O}}{(w_a - w_f) \times 0.99983} + 0.0012 \dots \text{g/cm}^3 \quad (1)$$

$$G = W(a) - W(fl) \quad (2)$$

Where: w_a = weight of solid in the air; w_f = weight of solid in the liquid;

G = buoyancy of the glass plummet; d = density

Pycnometer method is applicable to determinate the PPy particle density. This procedure is simple by using a know volume bottle, typically 25 ml. The measurement was done at 27.5°C.

$$\text{Solid sample of PPy} \quad \text{Sp.gr. } 27.5/27.5^\circ\text{C} = \frac{a \times d}{a + w - b} \quad (3)$$

where: a = mass of solid ; b = mass of pycnometer filled with water + solid at 23°C ;

e = mass of Pycnometer; d = sp.gr. 23/23°C of liquid;

w = mass of pycnometer filled with water

5.3.8 Morphology study

There are two steps for studying the morphology. Firstly, the admicellar synthesized PPy on NR particles obtained from solution after polymerization was observed by a transmission electron microscope (TEM, JEOL,2100). The magnification range was about 3000 -50 K.

Secondly, the morphology of the samples after polymerization and drying at 100°C for 6 hours was studied by SEM. The samples were taken into liquid nitrogen and then broken immediately to get cross section surface, and adhered to brass stubs. Next, the samples on the stubs were sputtered with a thin layer of gold. The mor-

phologies of the admicelled PPy/NR were observed by a scanning electron microscope (SEM, JOEL model JSM-5200). SEM digitized photographs were obtained with a magnification range between 1,500–5,000 times using an acceleration voltage of 15 kV.

5.3.9 Thermal properties measurement

Thermal stability, moisture content, and decomposition temperature of the admicelled PPy/NR were studied by a thermogravimetric-differential thermal analyzer (Perkin Elmer, Pyris Diamond, TG-DTA). The samples were weighed at 10-18 mg and put in a platinum pan. The instrument was set to operate at temperatures from 30 to 600°C at a heating rate of 10°C/min under nitrogen atmosphere, 100 ml/min.

5.3.10 Mechanical Properties Measurement

The mechanical properties for two specimen types were determined with one type (film shape) having a dimension of 20x100 mm (thickness 0.3-0.8 mm) as shown in Figure 5.4 Lloyd (UTM). The test was prepared by compression molding. The test followed ASTM D822-91 with a crosshead speed of 50 mm/min, a gauge length of 50 mm, and load cell 500 N under room temperature using Lloyd Universal Testing Machine, model :LRX. The test was repeated 5 times. The tensile strength test uses two clamps to hold the testing strip. When secured, the testing strip is pulled apart. The yield point and breaking point is then measured.

The other specimen type is the dumbbell shape, which had a thickness larger than 3 mm. the specific sample size (Figure5.4) was cut by using a pneumatic punch following ASTM D638M-91a. The samples were tested by using the Instron Universal Testing machine with a crosshead speed 50 mm/min, a gauge length of 13 mm, and load cell 100 kN under room temperature. The test was repeated 5 times.

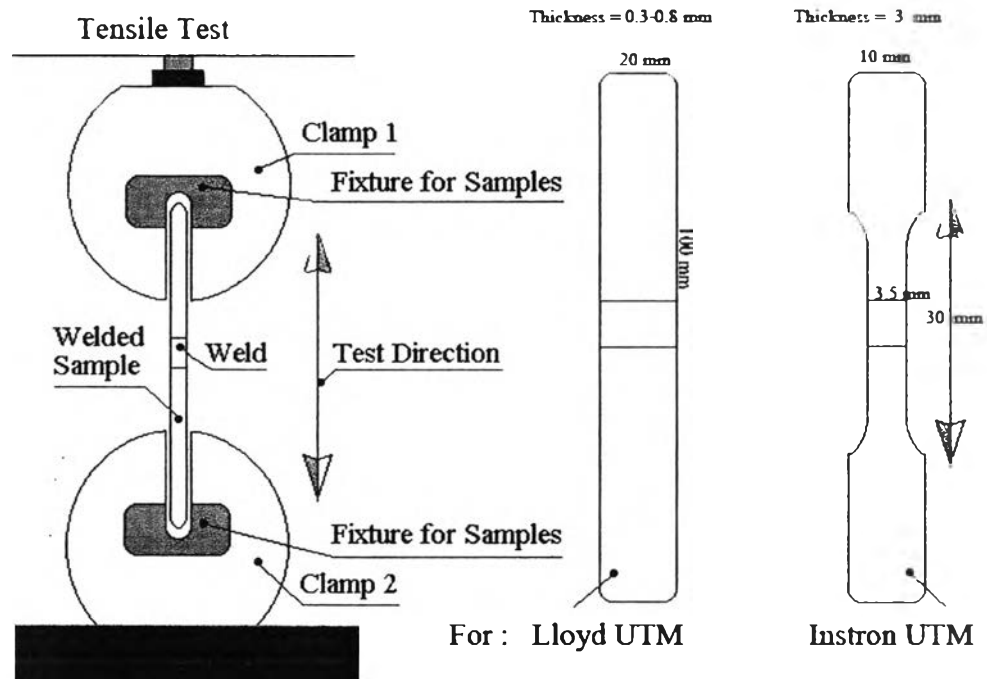


Figure 5.4 Preparation samples for tensile test.

5.3.11 Shore A and Shore D hardness Measurement

The flat specimen was placed on the plate. Then, the maximum height of the indenter was adjusted so that the tip of the indenter was approximately 10 mm above the test specimen. The unit was locked in position and the pointer was set to zero. The durometer probe was carefully, but fairly quickly and uniformly, lowered onto the test specimen. Then, initial shore hardness values were obtained by the pointer reading. According to ASTM D2240, the following conditions should be complied with :

- The test specimen should be at least 6 mm thick.
- The indenter should be at least 12 mm away from any edge of the specimen.
- At least 5 hardness readings should be taken per specimen.
- The instantaneous hardness reading on the dial gauge should be taken
- Only hardness values ranging between 10 and 90 are acceptable for shore A.
- If the value is greater than 90, the shore D test should be used instead.

5.3.12 Conductivity Measurement

The admicelled rubber films from compression (thickness 0.3-0.8 mm) were cut into a round shape with six inches in diameter and tested for their surface and volume resistivity by using a Keithley 8009 Resistivity Test Fixture and a Keithley 6517A Electrometer/High Resistance Meter. A dc voltage from 0.1 to 15 volts was applied to the specimen placed in the Keithley 8009 test fixture. Then, the current was read and the surface and volume resistivity were determined (ASTM D-257).

The resistance, R , of the films was calculated using Eq. 4, the volume resistivity, surface resistivity and the conductivity were found using Eqs. 5, 6 and 7, respectively:

$$R = \frac{V}{I} \quad (4)$$

$$\rho_v = \frac{22.9V}{tI} \quad (5)$$

$$\rho_s = \frac{53.4V}{I} \quad (6)$$

$$\sigma = \frac{1}{\rho_v} \quad (7)$$

where R is the resistance (watts), V is the voltage (volts), I is the current (amperes), ρ_v is the volume resistivity (ohm centimeters), ρ_s is the surface resistivity (ohm), t is the film thickness (centimeters), and σ is the conductivity (siemens per centimeter).

5.4 Results and Discussion

5.4.1 Preparation of Natural rubber sheet.

Natural rubber latex consists of particles of rubber hydrocarbon and non-rubber constituents suspended in an aqueous phase. These natural rubber particles can be separated from the aqueous phase by centrifugal method. The natural rubber particle can be grown to the various thicknesses on the anode (a working electrode, size 3.5x7 cm). Effect of voltage applied across the cell on the natural rubber sheet is clearly shown in Table 5.3, Figures 5.4 and 5.5, and Appendix D respectively.

Table 5.3 Effect of voltage on % yield and reaction times at Thiophene 100 mM(4.207g), NR latex(60%wt DRC) 25 g, and SDS 2.307g

Voltage	6	9	12	15
%yield	93%	94%	91%	90%
Times for synthesis (hr)	27	26	22	21

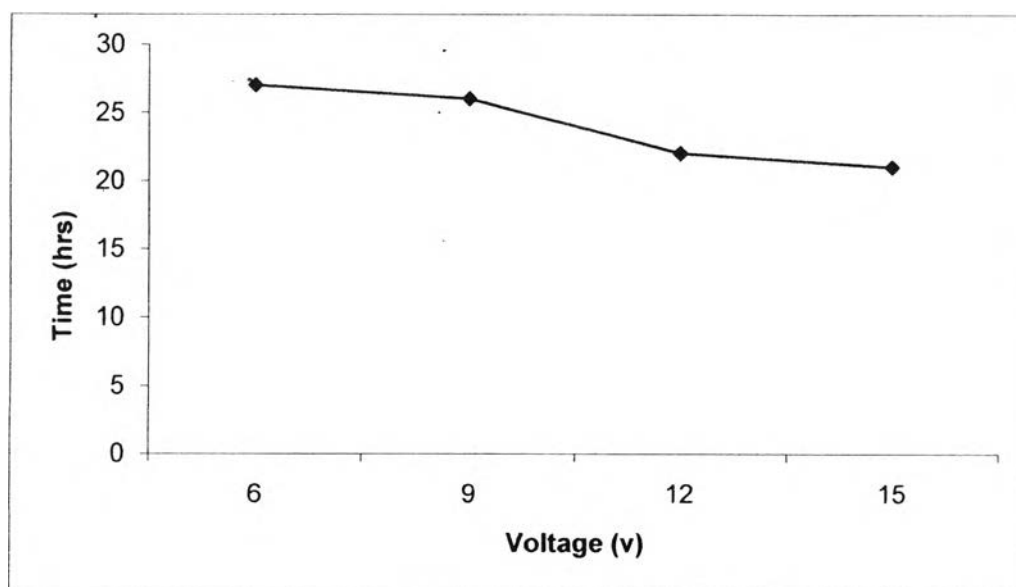


Figure 5.5 Effect of voltage applied on reaction time

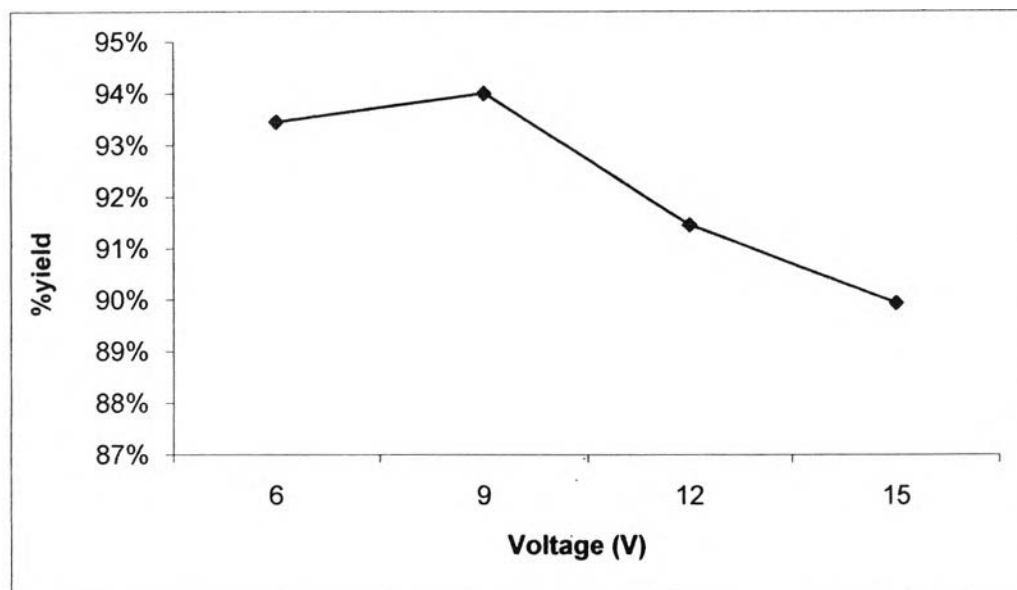


Figure 5.6 Effect of voltage applied on % yield.

Figure 5.5 shows the reaction time required to synthesize the admicelle rubbers; it was slowly decreased as the voltage increased. At higher voltage, the increment of thickness and yield were not smooth. It can be postulated that high voltage induced the faster deposition of negatively-charged rubber particles on the surface of the anode and the passivation or the over-resistance occurred on the anode at the same time. At highest voltage, 15V, the lowest yield was achieved as shown in the Figure 5.6. As a result, voltages greater than 9 volts does not enhance the best deposition, due to the lower in %yield. Therefore, a voltage of 9 volts was chosen as same as the condition of PPy in Chapter 4.

Next, the polymerization reaction was carried out for the admicellar polymerization of rubber with various Thiophene concentrations (20-800 mM) in the electrochemical method at 9V, 25°C. Table 5.4 shows the dependence of %yield and reaction times on the PTh concentration. It is also clearly shown in Figure 5.7 that %yield and reaction times of admicelled rubber were decreased along with the increased PTh concentration. The higher the concentration of PTh, the faster the reaction was.

Table 5.4 Effect of PTh content on % yield and reaction times at 9 V, NR latex (60%DRC) 25g, and SDS 2.307 g

PTh	(mM)	20	50	100	200	500	800
	(g)	0.841	2.104	4.027	8.414	21.035	33.656
Mass at anode (g)		23.67	24.23	25.81	29.70	39.43	48.91
%yield		91.59	89.39	88.92	88.88	85.65	83.38
Times (hr)		30	27	26	25	24	23

When : $\%yield = \frac{M_{total} \times 100}{(M_{NR} + M_{PTh})} : M_{sds}$ is not calculated because it can be removed by water

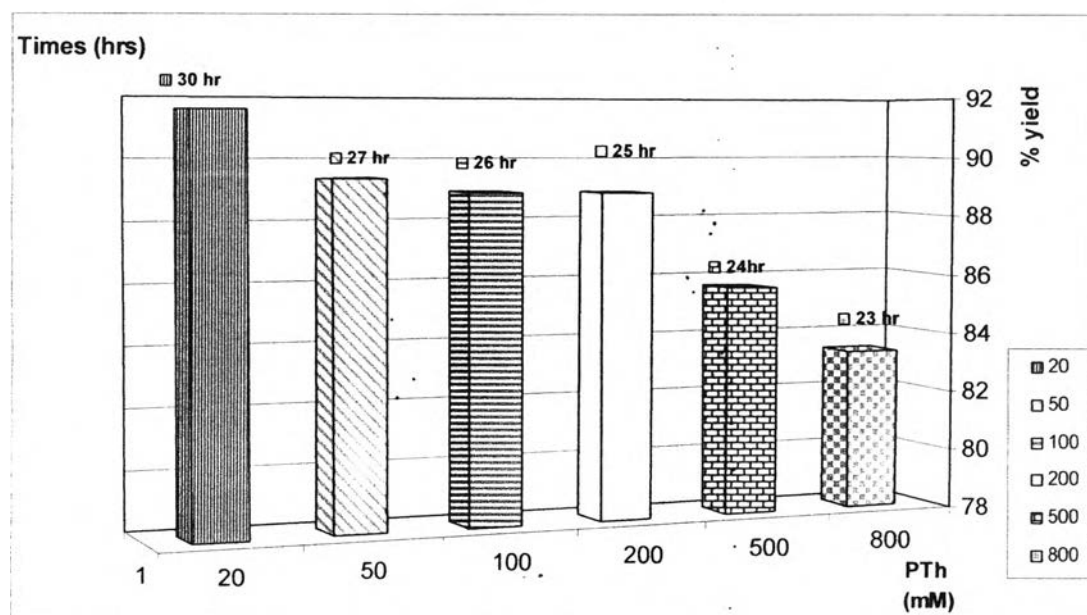


Figure 5.7 Effect of thiophene concentration on reaction times and %yield

Admicelled rubber was slowly deposited at the anode electrode as shown in Figure 5.8 and Appendix D. The success of polymerization can be determined the rate equation of accumulated mass at the anode electrode as below:

$$A2 : y=7.69\ln(x) + 0.79 \quad (5)$$

$$A5 : y=8.21 \ln(x) - 1.44 \quad (6)$$

$$A10 : y=8.89 \ln(x) - 1.58 \quad (7)$$

$$A20 : y=10.63 \ln(x) - 2.49 \quad (8)$$

$$A50 : y=14.75 \ln(x) - 4.51 \quad (9)$$

$$A80 : y=18.55 \ln(x) - 8.58 \quad (10)$$

Finally, the solution changed to a clear solution, indicating that the polymerization was completed. Then, other properties were observed

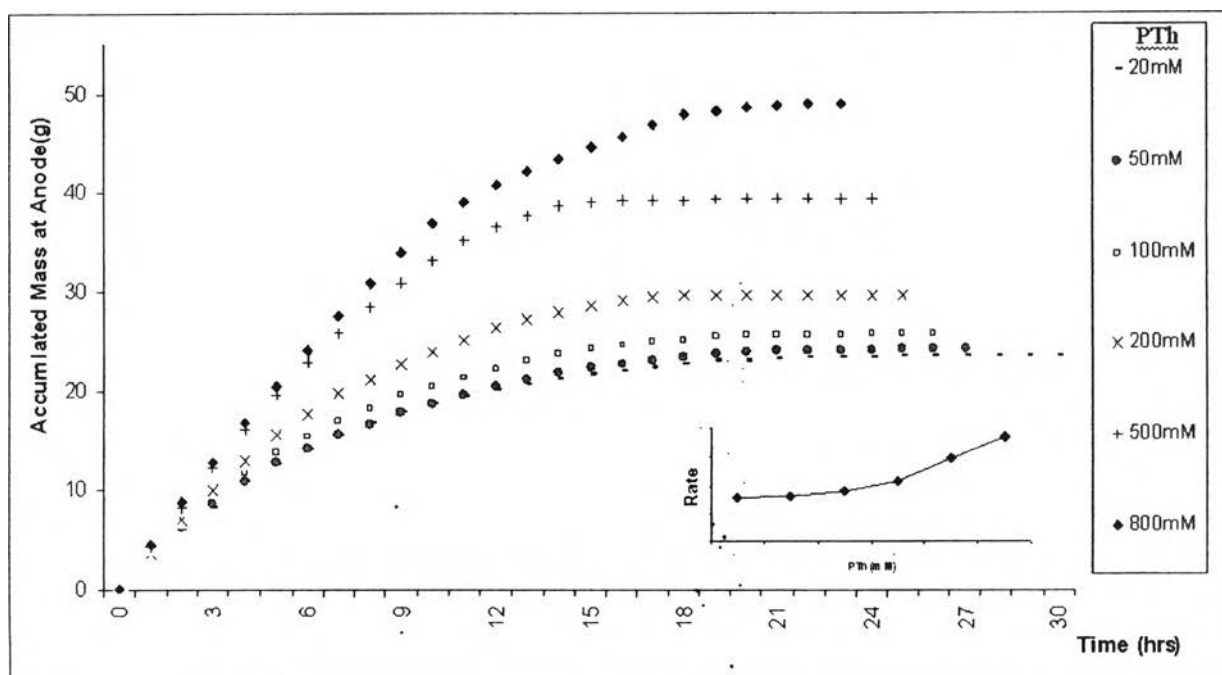


Figure 5.8 Accumulate weight equation of admicellated rubber (PTh: NR).

Reaction conditions to induce high electrical conductivity of conductive natural rubber were studied in order to select the optimum conditions. The major parameters that influence the quality of conductive rubber prepared with various concentrations of PTh, 9V, 25°C is pH value. Bunsomsit, K et.,al (2002)¹⁰ studied the point of zero charge. The point of zero charge or net surface charge of zero is known from the intersection of the electrophoretic mobility curve and the zero axis. When the pH of the solution is equal to PZC, the surface charge of the substrate is equal to zero. At pH values below the PZC, the substrate surface exhibits a positive charge, then anionic surfactants are adsorbed, or vice versa. In this study, the pH was adjusted to be less than 3.0 and the pH values were determined every hour until the clear solution obtained. The result is shown in Figure 5.9 and Appendix E (Table E2).

Effect of pH on reaction times is shown in Figure 5.9. It is clear that the pH value increases with increasing reaction time. This is probably due to the preferred basic condition generated by the high conversion to PTh. This effect agrees with the reported by K.S. Jang (2004)¹⁵⁶. Moreover, the correlation at low pH can be en-

hanced the conductivity due to severe protonation of the polymer backbone. On the other hand, the significant conductivity drop in the high pH range may be attributed

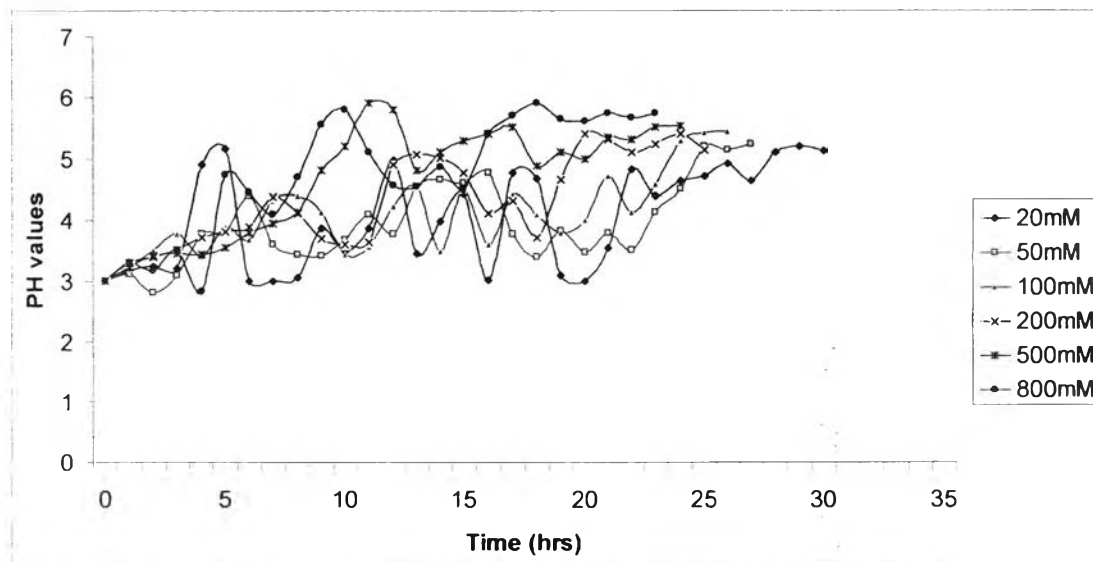


Figure 5.9 Effect of reaction times on pH values of PTh solution

5.4.2 Fourier-Transform Infrared Spectroscopy of Admicelled NR Latex

The infrared spectra of pure rubber, pure PTh, and admicelled rubbers in the region from 4000 to 400 cm^{-1} are shown in Figures 5.10– 5.13.

The obtained spectrum of pure Thiophene (Figure 5.10) agrees with the IR spectrum reported by M. Emin Kumru et al. (2001)⁹⁴. As shown in Figure 5.10, there are characteristic bands belong to aromatic rings. There are: C-H stretching band at 2958-2919 cm^{-1} ; C-C and C=C stretching band at 1645-1522 cm^{-1} ; CH_2 in plane deformation band at 1469-1377 cm^{-1} and C-H in plane deformation band at 1209-1069 cm^{-1} . The band at 828 cm^{-1} corresponds to C-H out of plane deformation (James.L et al. 2006)¹⁰⁷. The band at 720 cm^{-1} assigns to typical C-S bending band (Bekir.S et al. 2003)⁷⁹. IR spectrums of PTh are summarized in Table 5.5.

The obtained spectrum of pure rubber (Figure 5.10) confirms with the IR spectrum reported by Rippel M., *et al.* (2003)¹⁰. The band at 3036 cm^{-1} corresponds to =C-H stretching. Bands at 2960, 2915, and 2853 cm^{-1} are assigned to the C-H stretching of CH_3 , the C-H stretching of CH_2 , and C-H stretching of CH_2 and CH_3 , respectively. The principle peaks corresponding to isoprene functional groups of natural rubber are observed at 3036, 2960, 2915, 2853, 1662, 1448, 1375, 1129, and 834 cm^{-1} . Several other peaks that are not associated with isoprene are also present: an intense broad band between 3200, 3500 cm^{-1} indicating the presence of a hydroxyl group, and an amide (N-H) peak at 3280 cm^{-1} (more apparent in cream rubber), a carbonyl (C=O) peak at 1737 cm^{-1} , a small amide (N-H) peak at 1548 cm^{-1} (both more apparent and more resolved in cream rubber), and a series of peaks between 1130 to 1010 cm^{-1} , indicating oxygenated compounds. The peak at around 1080 cm^{-1} is assigned to two categories: polyisoprene units and proteins/phospholipids (Rippel M., *et al.* 2003)¹⁰⁶. IR spectrums of NR are summarized in Table 5.6.

The FT-IR spectra of all admicelled rubbers reveal the combined absorption of rubber and PTh. These results confirm the existence of PTh after polymerization in the rubber system. The absorbance of NR decreases as PTh content increases as shown in Figure 5.12-5.13 and IR spectrums are summarized in Table 5.7.

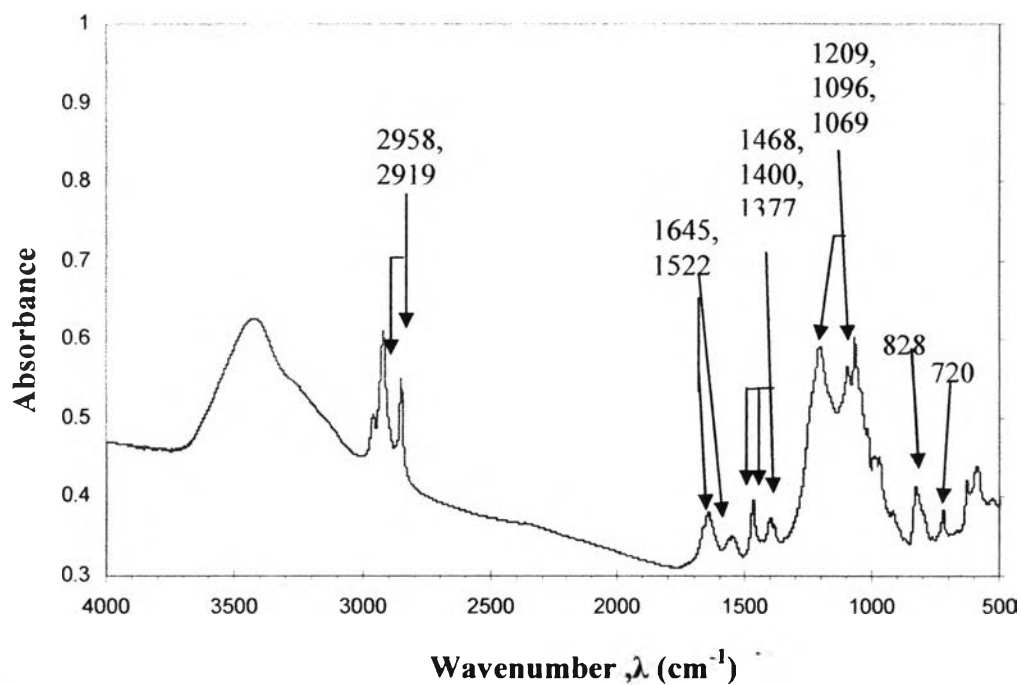


Figure 5.10 FT-IR spectrum of Polythiophene

Table 5.5 Assignment for the FTIR spectrum of thiophene^{94,106}

Wavenumber, λ (cm^{-1})	Assignment
2958,2919	C-H stretching
1645,1522	C=C and C-C stretching
1468, 1400, 1377	CH ₂ deformation
1209,1096,1069	C-H in plane deformation
828	C-H out of plane deformation
720	C-S bending

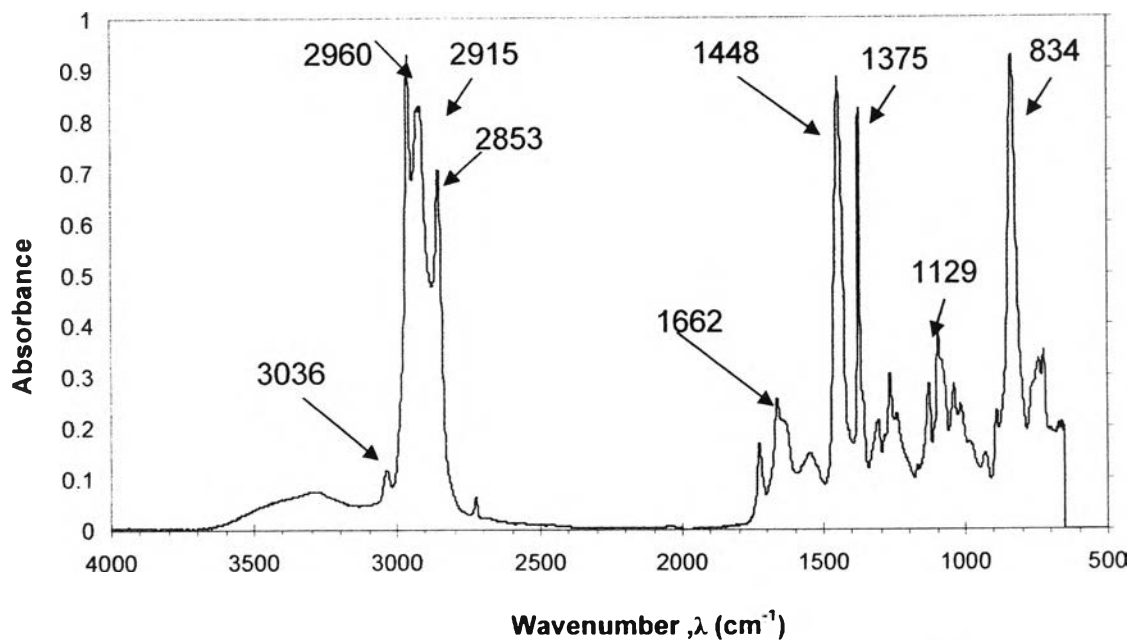


Figure 5.11 FTIR spectrum of pure natural rubber, Polyisoprene.

Table 5.6 Assignment for the FTIR spectrum of isoprene¹⁰⁶

Wavenumber, λ (cm ⁻¹)	Assignment
3036	=CH stretching
2960	C-H stretching of CH ₃
2915	C-H stretching of CH ₂
2853	C-H stretching of CH ₂ and CH ₃
1662	C=C stretching
1448	C-H bending of CH ₂
1375	C-H bending of CH ₃
1129	C-H bending
834	C=CH wagging

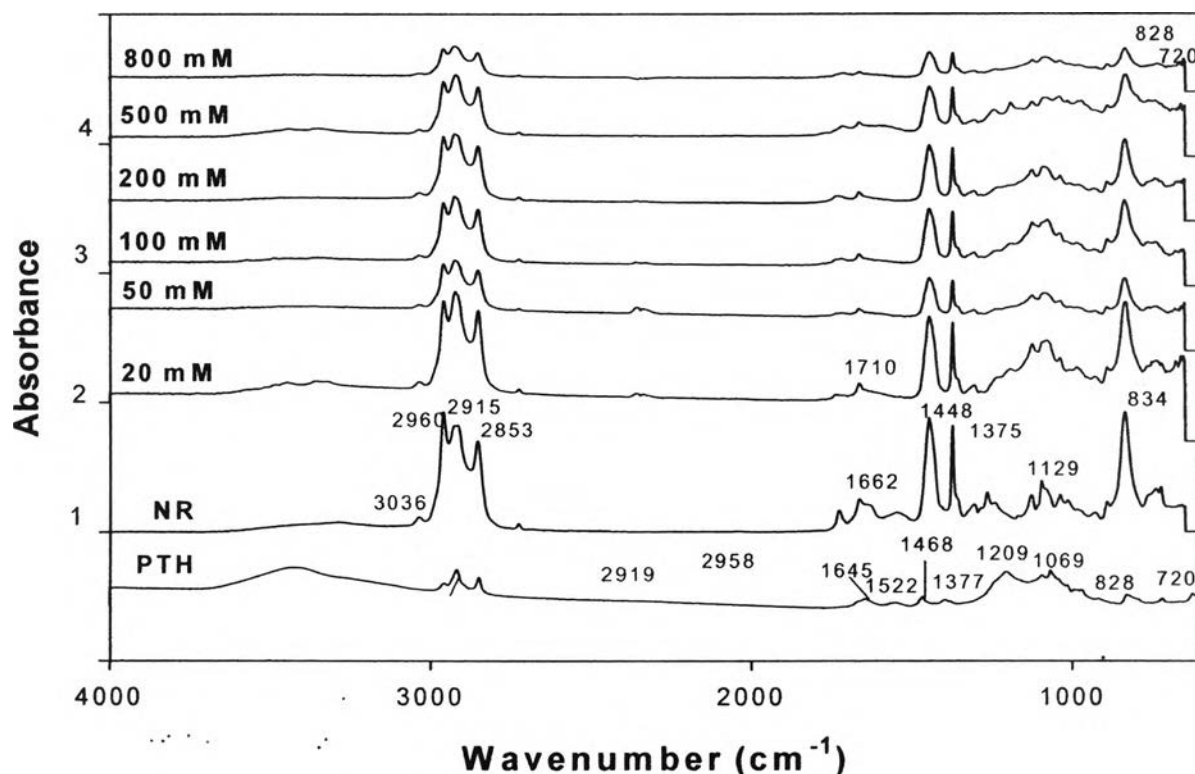


Figure 5.12 FT-IR spectra of the admicelled rubbers with polythiophene (HATR flat plate system with 45 °C ZnSe crystal).

Table 5.7 Assignment for the FTIR spectrum of combination^{9,10,11,12,13,14}

Wavenumber, λ (cm^{-1})	Assignment
2958, 2919	NH stretching (PTh)
2950, 2915, 2853	CH stretching (NR)
1710, 1645, 1558, 1522	C=C stretching (NR+PTh)
1490, 1468, 1400, 1350, 1209	CH and CH ₂ in plane bending (NR+PTh)
828	CH out of plane deformation
720	C-S bending band

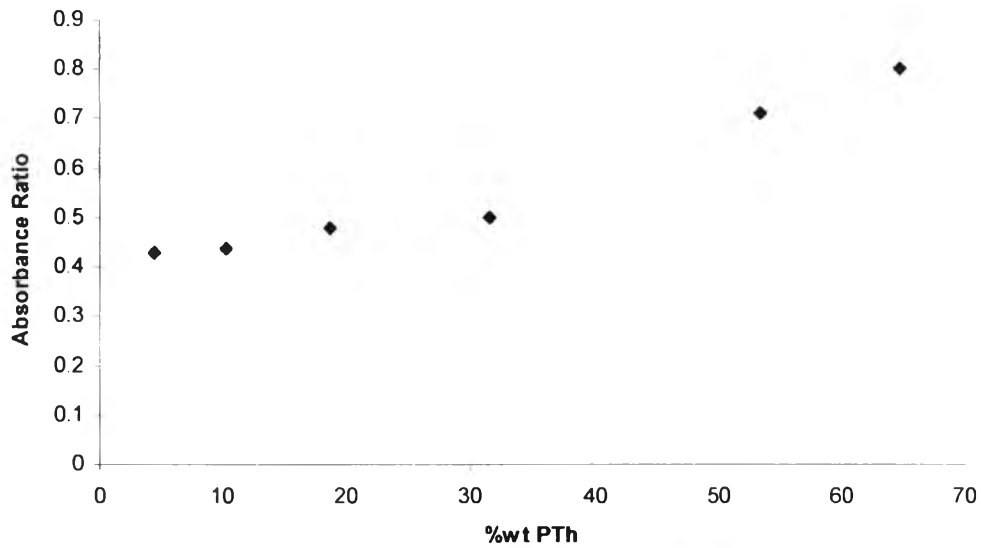


Figure 5.13 The Absorbance ratio (720cm^{-1} (PTh) / 2915cm^{-1} (NR)) at difference concentration.

5.4.3 Density measurement

To further understand the change of properties in NR/PTh composites. The experiment will focus in more detail in the density. Density of specimens was measured using the Sartorius approach, model :YDK01, where the sample weight in air and then in the water with a balance with a reproducibility of better than $10\ \mu\text{g}$. Each reported measurement represented the average of at least 3 specimens which calculate by using the following equation:

H₂O	0.9964	(from table)
temperature	27.5	

$$\text{Eq } d = \frac{w_a \times d_{H_2O}}{(w_a - w_f) \times 0.99983} + 0.0012 \dots \text{g / cm}^3$$

$$G = W(a) - W(fl)$$

w_a = weight of solid in the air

w_f = weight of solid in the liquid

G = buoyancy of the glass plummet

d = density

Pycnometer method is applicable to determinate the PPy and PTh density. This procedure is simple by using a know volume bottle, typically 25 ml. The measurement has to carried out at a certain temperature by filling the liquid sample in the pycnometer bottle unit it is full and cap is put on. At this point the volume of liquid sample is equal to the bottle volume, i.e. 25 ml. Then the bottle is cleaned and weighed to a constant weight. Density is then calculated; divided measured weight by bottle volume. It shows more details in Appendix I and Table I-1.

The density of admicelled NR increases gradually with PTh content (Figure 5.13), the abrupt change in density is found at 800 mM PTh. In addition, the results show that the admicelled NR samples have densities lower than 1 (unity) and higher than that of NR but higher that of PTh and thiophene monomer. This suggests the admicelled NR is light although the dense pack of PTh is observed. As observed in the Table 5.8, both of experimental and calculation of density are nearly same results. The increase in the density of PTh becomes form PTh tiny globules (at low amount of PTh) to reside, which explains the same reason by using TEM. The PTh tiny globules was also surrounded the NR particles and in the swollen region. This interesting to note that as PTh content increase ($\geq 100\text{mM}$) the tiny globule packing becomes denser, as a result, the rough surface coating become smooth coating and packing as layers.

Thus, the admicelled rubber particles have more opportunity to contact each other. As the volume fraction of PTh increased to the critical value, the conductivity mechanism of PTh in the polymer changes from the tunneling effect to direct contact, and the conductivity of the polymer composites increase dramatically. These changes in conductivity are present in Appendix G and Section 5.4.9.

Thus, the higher number of polymer chains was obtained when content is high to abstract electron from thiophene and enhance free radical polymerization, resulting in higher conductivity and higher in their density.

Table 5.8 measurement density of conductive polymer

Sample	w. air	w. fl	G	$d_{\text{experimental}}$	$D_{\text{calculation}}^{**}$	$d_{\text{calculated of PTh}}^{***}$
Rubber	0.2810	-0.0291	0.3112	0.9011 ± 0.028	0.9011	-
Rubber (centrifuge)	0.2837	-0.0301	0.31379	0.9022 ± 0.018	0.9022	-
20	0.2810	-0,0291	0,3112	0.9068 ± 0.0224	0.9092	1.0059
50	0.2837	-0,0301	0,31379	$0.9138 \pm 0,023$	0.9187	1.0235
100	0.2121	-0,0213	0,2334	0.9249 ± 0.0332	0.9322	1.0360
200	0.2371	-0,0218	0,2589	0.9428 ± 0.0144	0.9528	1.0438
500	0.2198	-0,01732	0,23712	0.9774 ± 0.0339	0.9882	1.0531
800	0.2120	-0,01236	0,22436	0.9973 ± 0.0213	1.0064	1.0576
Thiophene				1.063	1.0630	-
PTh				1.0794*	1.0794	-

* Measurement the density of solid particle by using Pycnometer (in appendix I)

Calculation density from %wt and *Calculation the density of PTh in specimens (in appendix J)

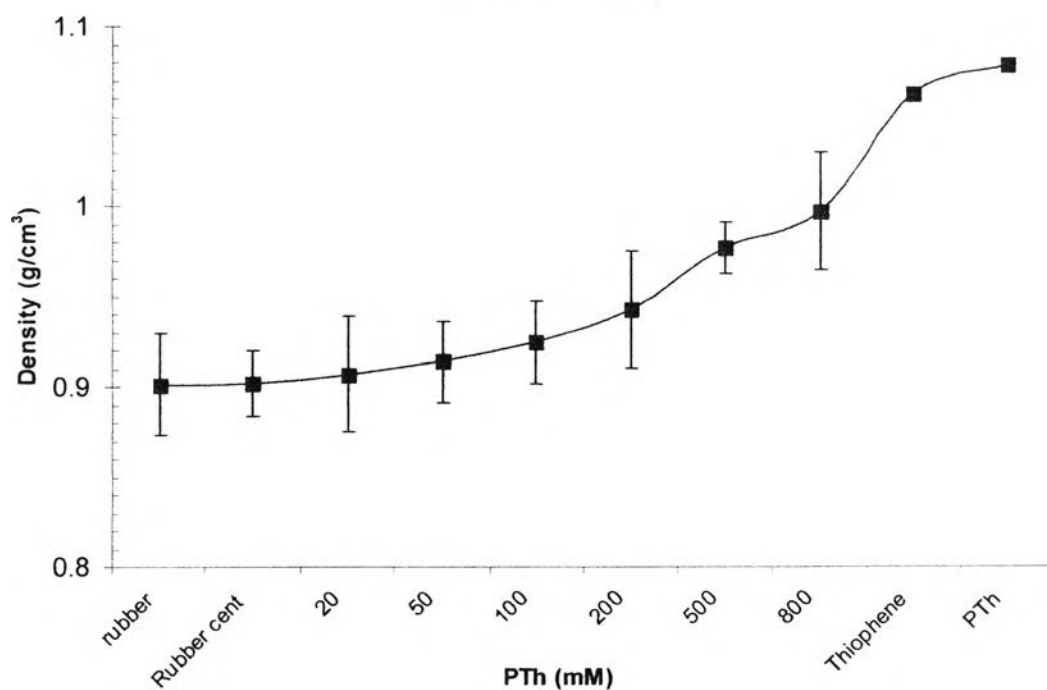


Figure 5.14 Variation of density with polythiophene concentration for admicellar rubber

5.4.4 Particle Size Distribution of NR Latex

The particle size distribution of NR latex before admicellar polymerization showed the mean diameter $1.05 \mu\text{m}$ and the mean specific surface area $6.874 \text{ m}^2 / \text{g}$. These results indicated the polydispersity of NR latex particles with narrow size distribution (Figure 5.15).

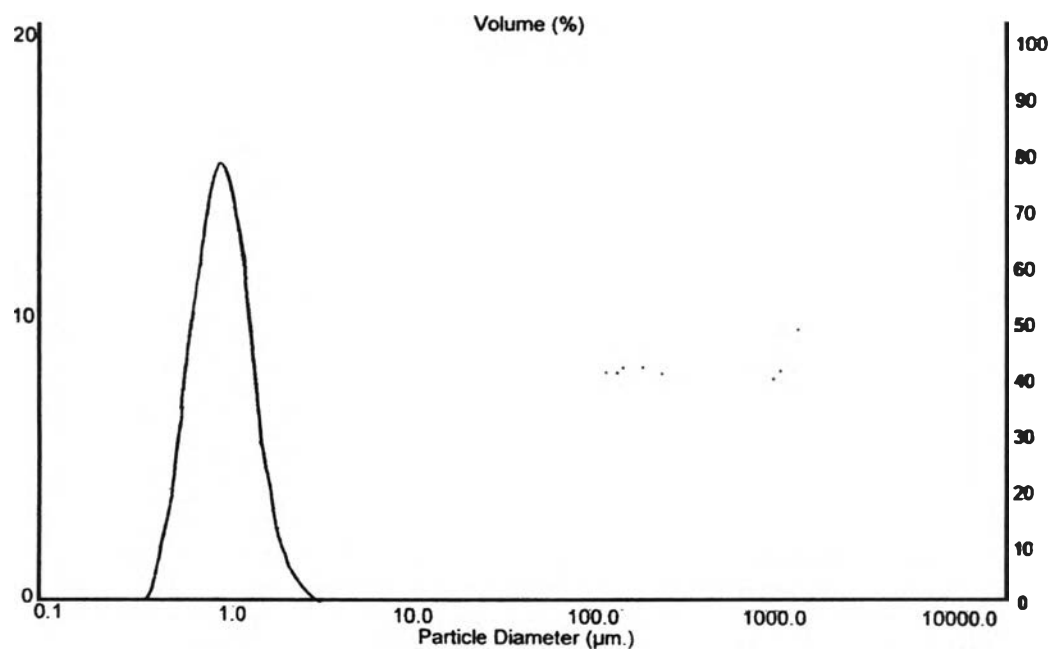


Figure 5.15 Histogram showing the particle size distribution by volume of the natural rubber latex.

5.4.5 Transmission Electron Microscopy (TEM) ^[96-98]

The morphologies of the admicelled rubbers were investigated by transmission electron microscopy (JEOL-JEM 2100) at 200 kV. The TEM micrographs of the admicelled rubber with different PTh concentrations reveal the round shape of rubber particles with an evenly coating conductive polymer over the particles. The sample shows latex particles coated by SDS, and the PTh layer as a core-shell structure where the NR particle is the core and PTh is the shell. The samples, natural rubber, with 20, 50, 100, 200, 500, and 800 mM of polythiophene clearly show coating of PTh on each latex particle individually, as shown in Figures 5.16-5.24. The average core particle diameter was estimated to be between 0.5 and 0.9 μm and the coating particles were between 0.8 and 2 μm .

Figure 5.16 shows the primary particles of thiophene, size diameter about 30-40 nm. They form into globular aggregates with rough surface of 100-250 nm. Figure 5.17(left) shows NR particles with no OS staining, it reveals that as particle becomes bigger and darker especially in the centre and lighter at the outer part, suggesting the sphere shape. The minimum size is $\sim 0.1 \mu\text{m}$ while maximum is almost $\sim 2 \mu\text{m}$. The boundary of NR particle becomes smear with SDS adsorption as shown in Figure 5.18(left).

As shown in Figure 5.18-5.24 the round smooth surface still preserved for the SDS admicelled NR particles, when PTh was admicelled polymerization on NR. It confirmed that PTh-SDS-NR nanoparticles shows spherical structure similar to sulfonated polythiophene nanoparticles by studied Yasemin.A et al.(2005) ⁹⁶.

After washing to remove outer SDS layer the round shape was also seen, but its boundary is swollen into greater distance allowing PTh tiny globules (30-90nm) to reside. The PTh tiny globules was surrounded the NR particles and in the swollen region. This interesting to note that as PTh content increase ($\geq 100\text{mM}$) the tiny globule packing becomes denser, as a result, the rough surface coating become smooth coating. This reveals the ultimate incorporation of PTh in NR at nanometer level. In addition, the dense packing of PTh globular should also attribute to the fast reaction when higher PTh content is used.

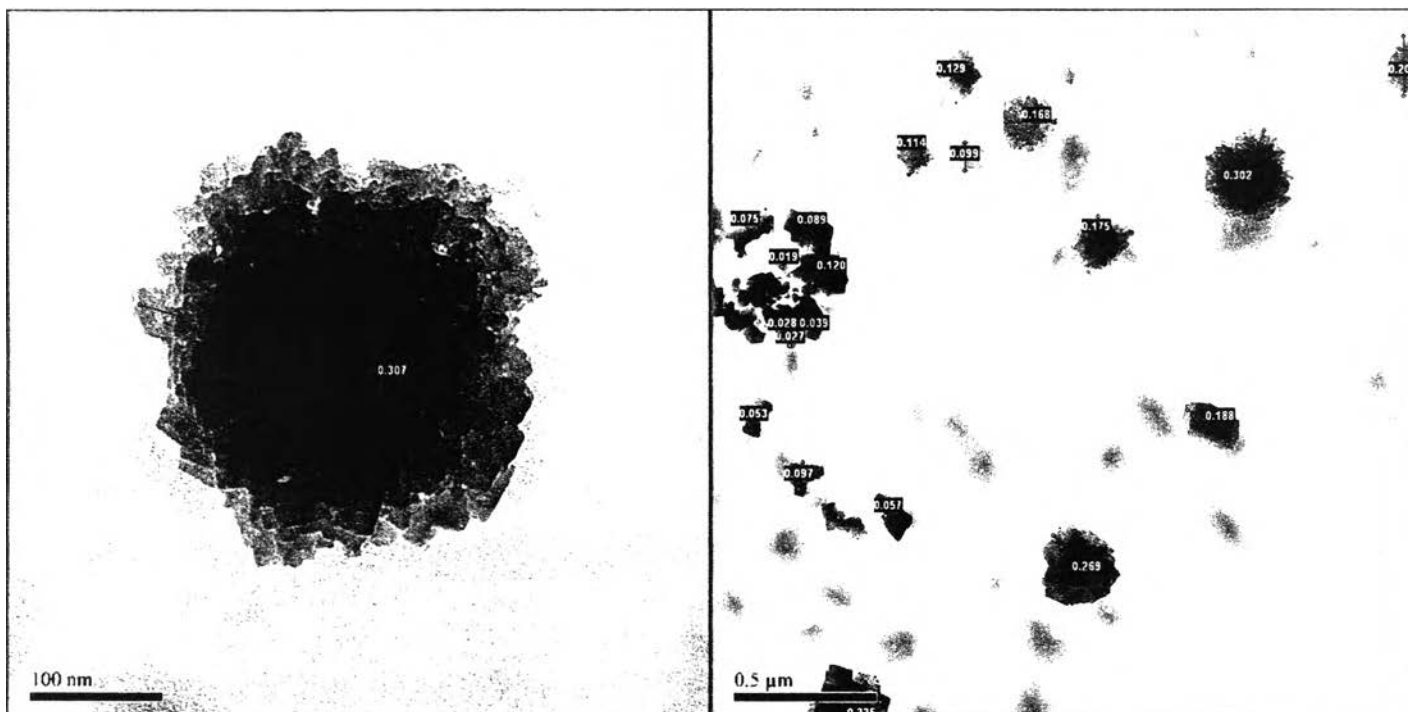


Figure 5.16 Transmission electron microscope (TEM) of PTh

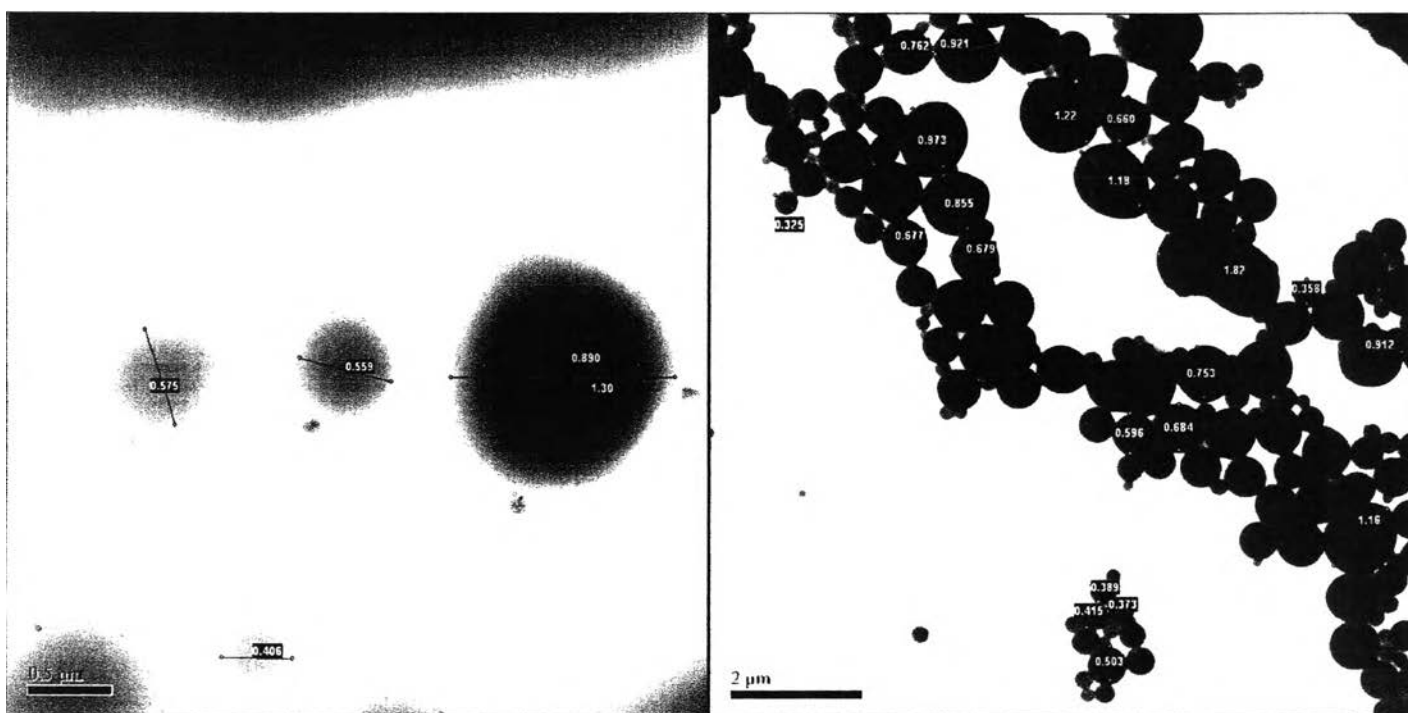


Figure 5.17 Transmission electron microscope (TEM) image of the natural rubber latex and no OS (left), with OS (right)

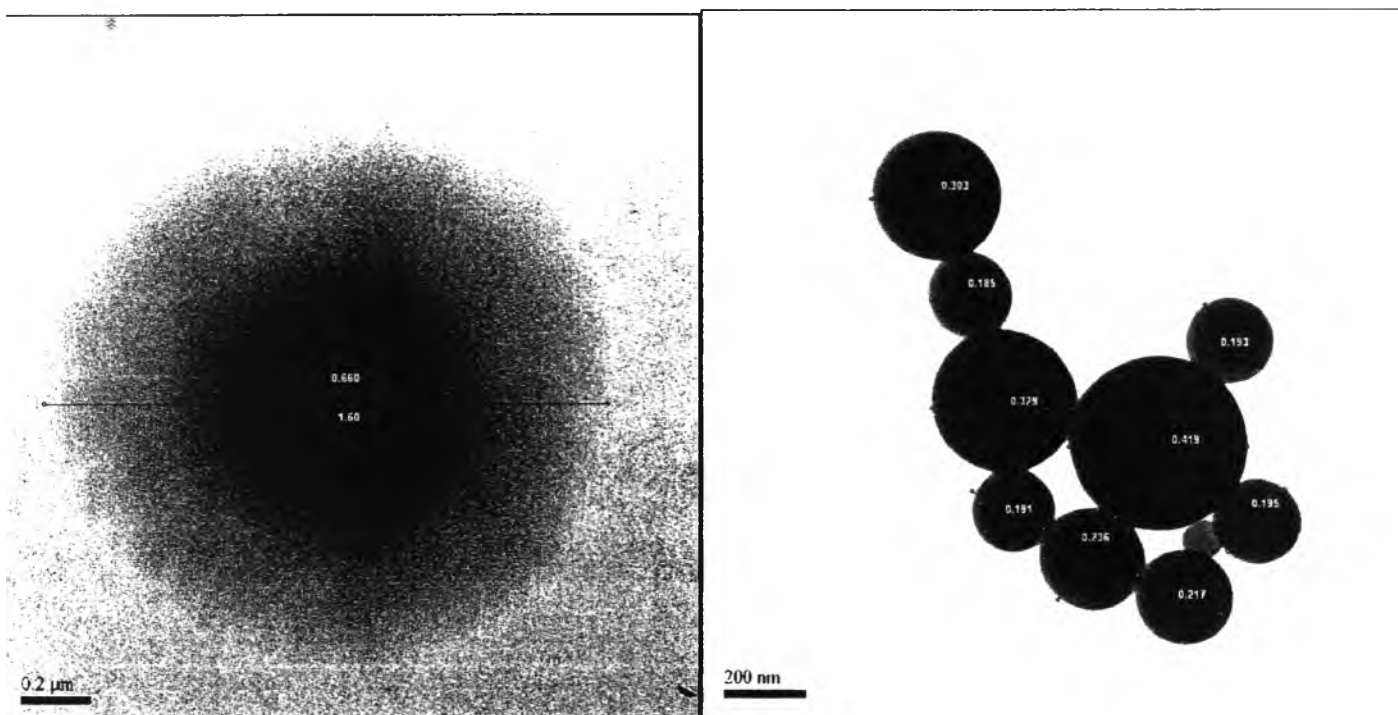


Figure 5.18 Transmission electron microscope (TEM) image of the coated admicelled rubber with Sodium Dodecyl Sulfate (SDS) as a bilayer form, no OS (left), with OS (right).

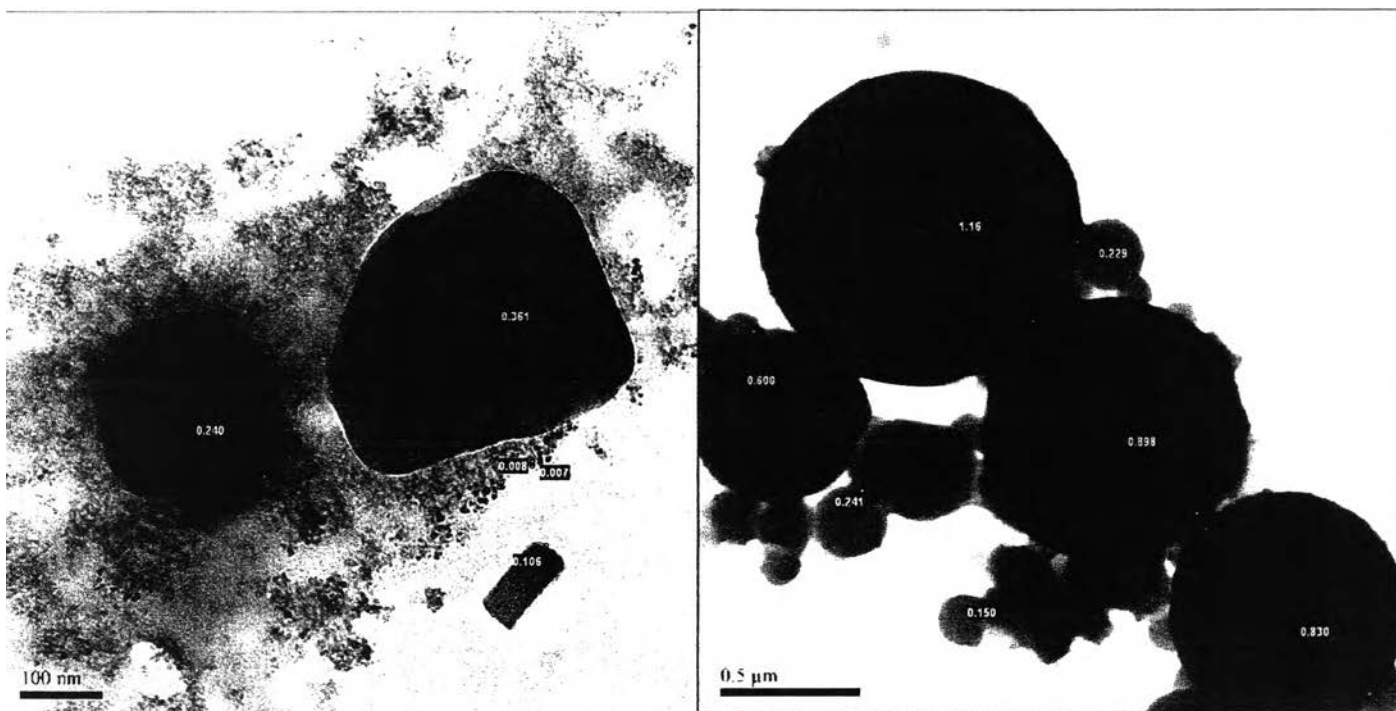


Figure 5.19 Transmission electron microscope (TEM) image of the coated admicelled rubber (with 20 mM PTh) by using the electrochemical method.

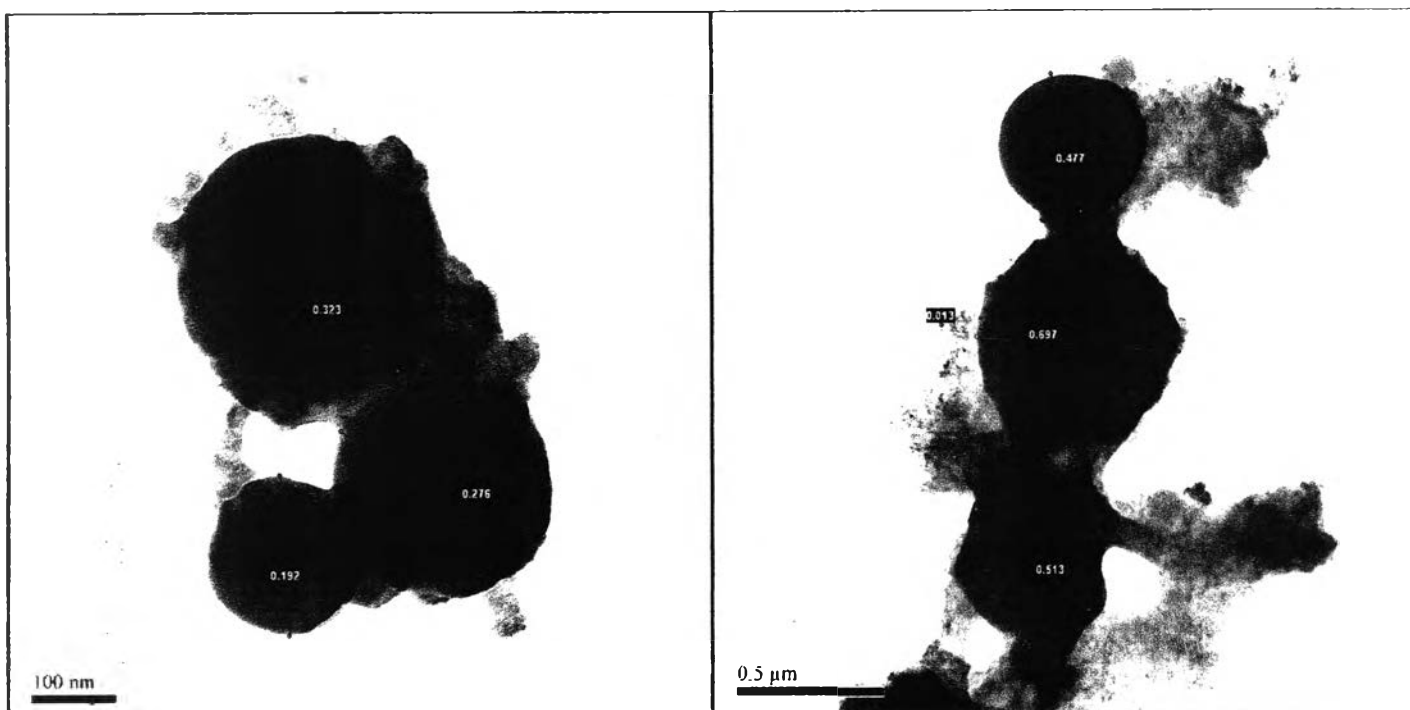


Figure 5.20 Transmission electron microscope (TEM) image of the coated admicelled rubber (with 50 mM PTh) by using the electrochemical method.

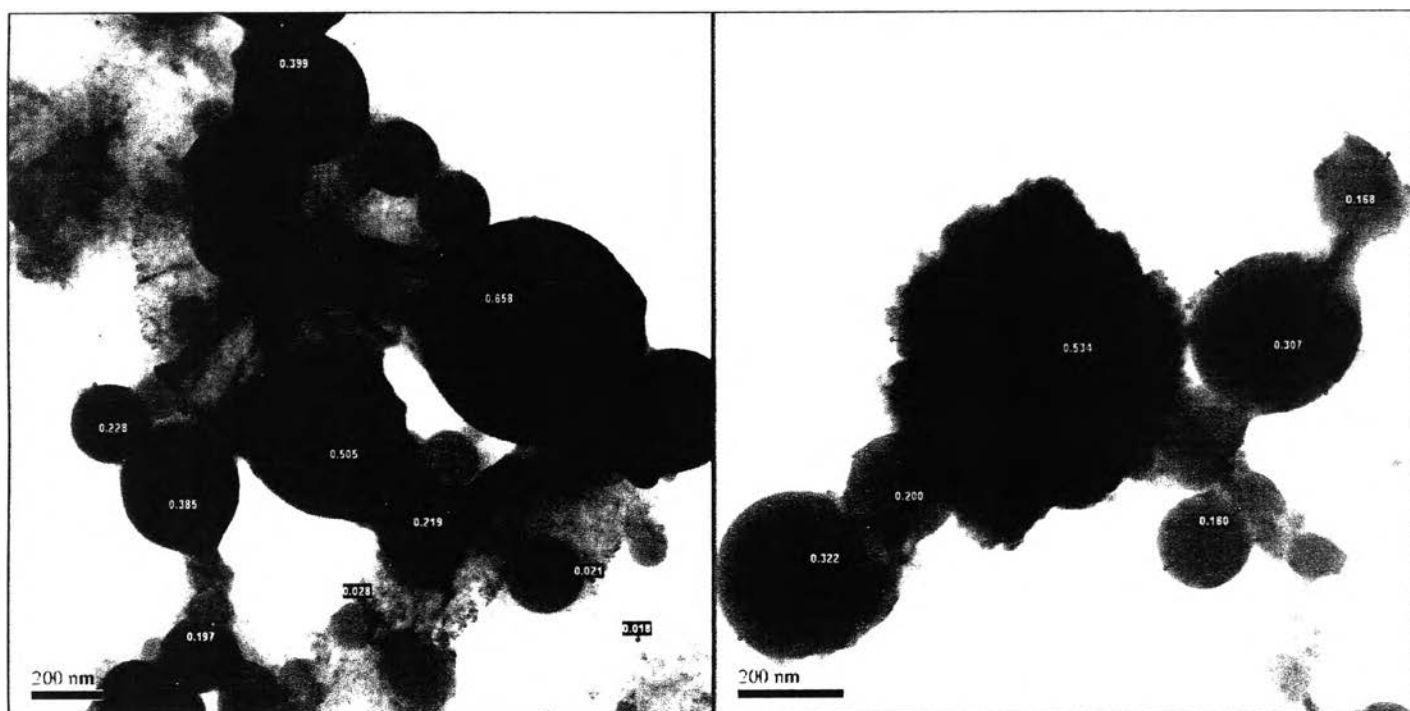


Figure 5.21 Transmission electron microscope (TEM) image of the coated admicelled rubber (with 100 mM PTh) by using the electrochemical method.

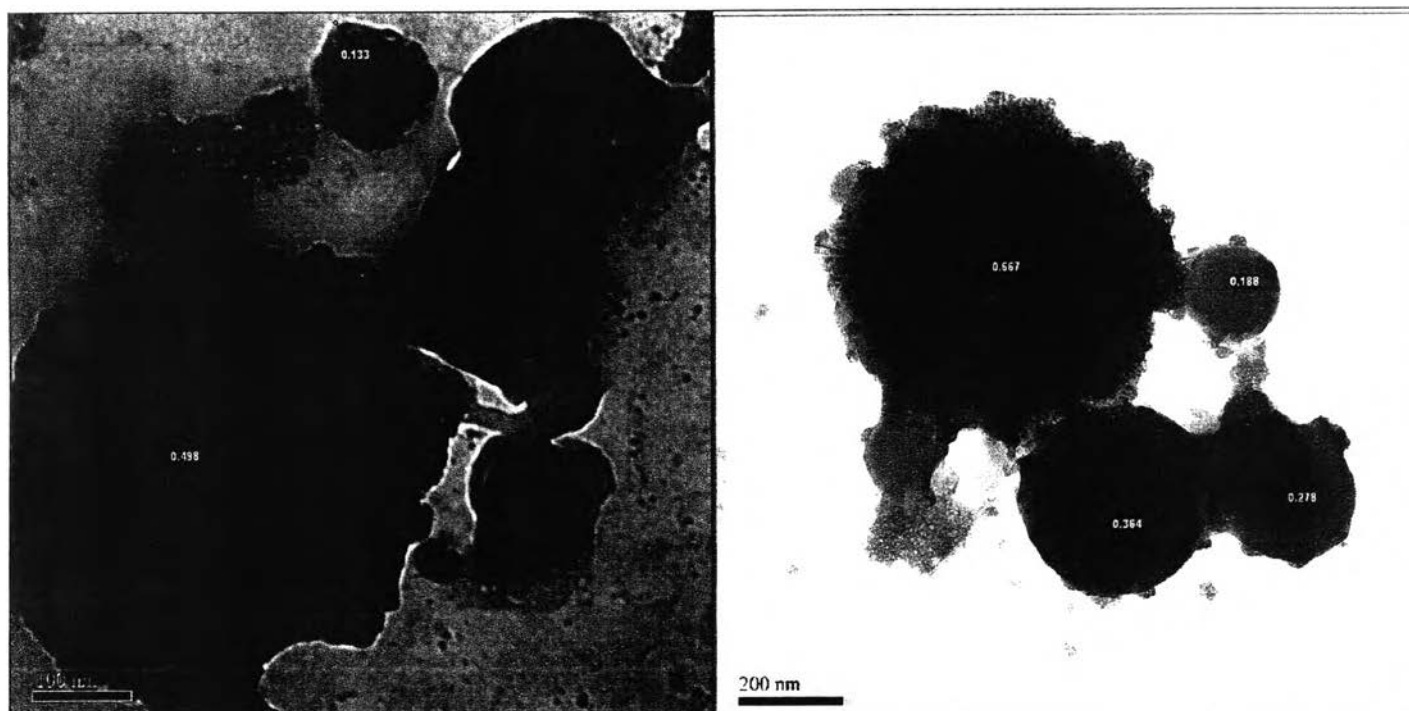


Figure 5.22 Transmission electron microscope (TEM) image of the coated admicelled rubber (with 200 mM PTh) by using the electrochemical method.

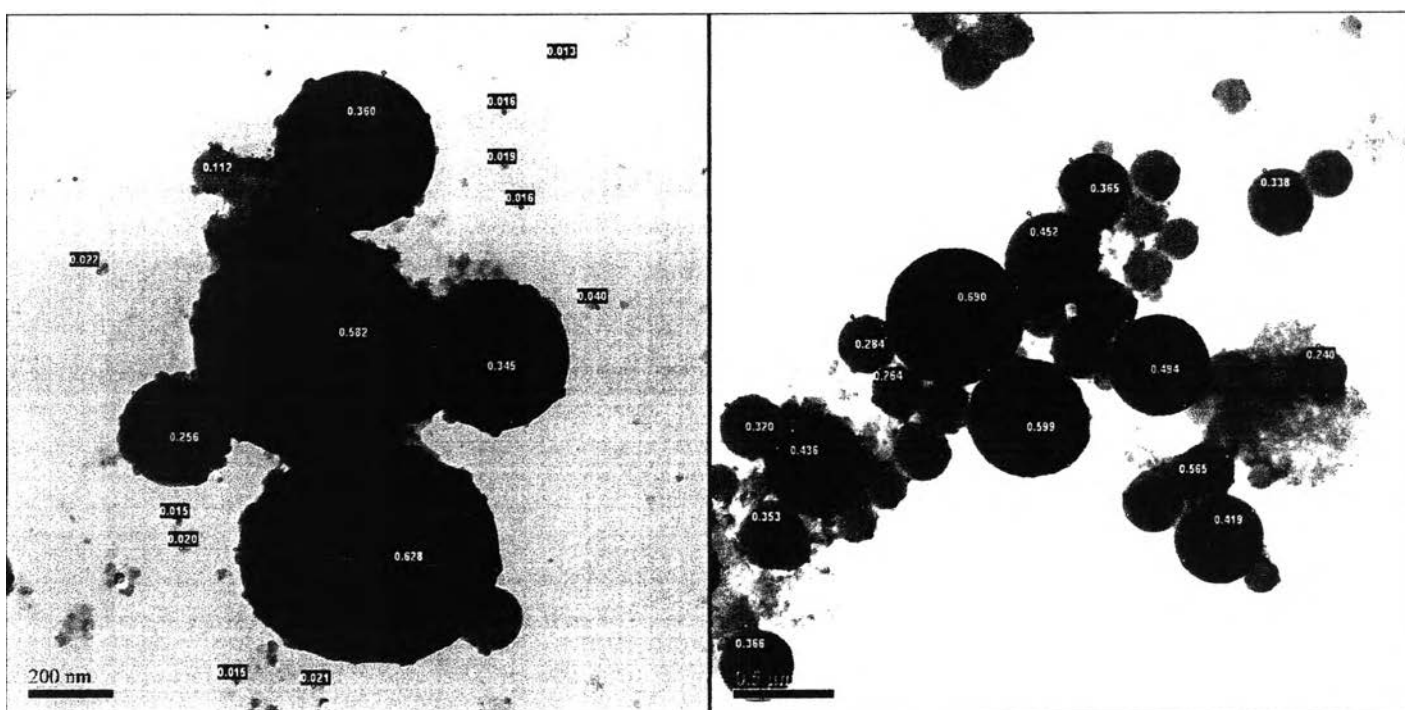


Figure 5.23 Transmission electron microscope (TEM) image of the coated admicelled rubber (with 500 mM PTh) by using the electrochemical method.

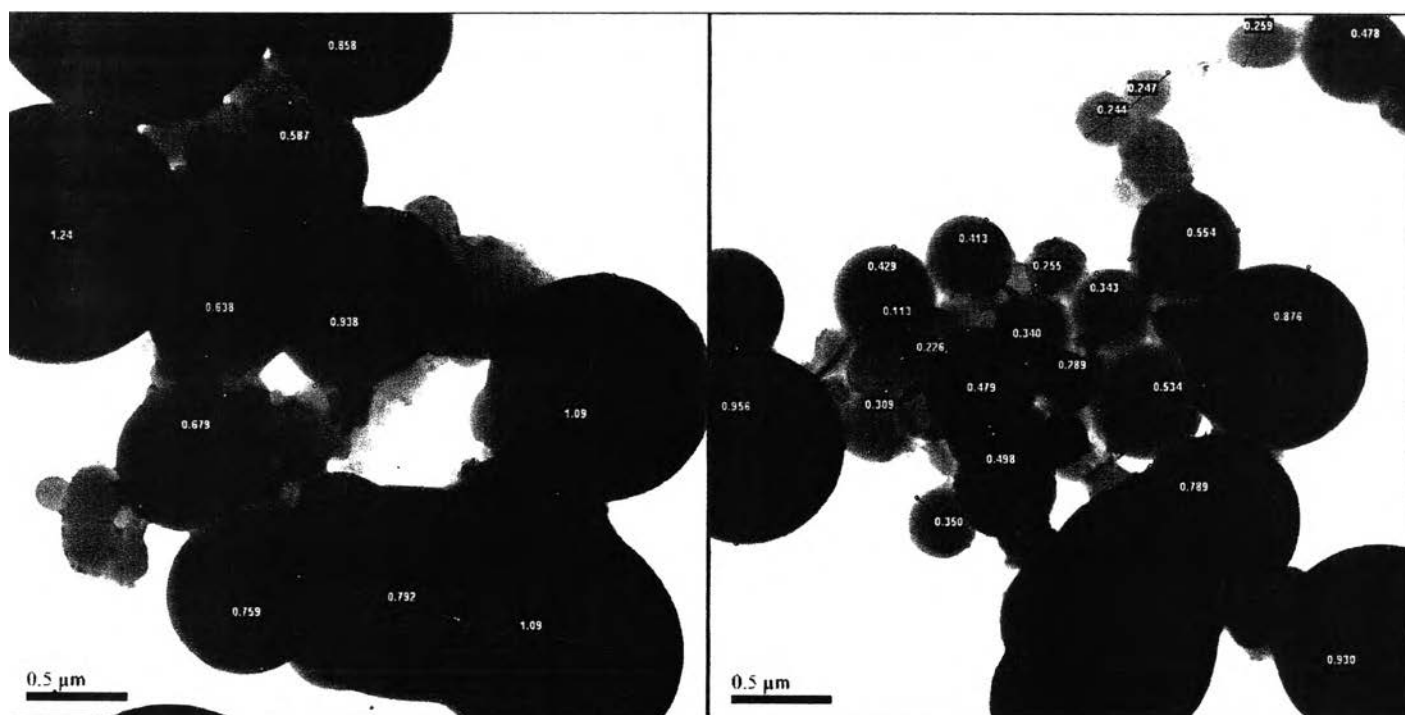


Figure 5.24 Transmission electron microscope (TEM) image of the coated admicelled rubber (with 800 mM PTh) by using the electrochemical method.

5.4.6 Scanning Electron Microscopy ^[91,92,93,94]

The morphologies of the PTh-admicelled rubbers were investigated by scanning electron microscopy. The SEM result can confirm the presence of polythiophene. As observed in Figure 5.25, a grained texture of thiophene is present and it demonstrated spong-like, pores, rigid-rod-like structure and globular structure with particle size about 1 μm . The surfactant additives can result in the morphology of PTh. Interesting morphologies were also obtained for PTh prepared in the different surfactants ^[158-159]. The morphology of PTh in the presence of anionic surfactant was similar to the studied characterization by Gok.A (2007) ⁹². The presence of different surfactant with PTh showed significantly different morphology. At the same concentration ratio, surfactant-free PTh has a globular structure with particle size about 1 μm , but some fibrils are presented. PTh-DBSNa (Anionic type) reveals an interesting ribbon structure. PTh-TTAB (Cationic type) is shown the layer structure. PTh-Tween20 (non-ionic type) is shown the smooth surface with small deformed globules. Surprisingly, PTh-SDS is present as tiny particles (globules) which becomes a continuous or matrix layer as rigid-rod-like structure (Figure 5.25). In addition, NR exhibited the smooth surface without any coating as shown in Figure 5.26.

A comparison of the SEM micrographs corresponding to the various concentrations of PTh (Figure 5.27-5.32) point out that the morphological structures of the surface are different shapes and sizes. A core-shell structure is appeared where NR particles are the core and PTh is the shell. The sample with 20 mM PTh shows small deformed globular latex particles coated by PTh and it becomes a continuous or matrix as layer of rigid-rod-like structure. It also has pores and cracks along the substrate. One reason might be due to less cross-linking between the PTh and the substrate, which make it easy for cracks to appear because of the evaporation. The arrangement matrix was also possible overlap each other as shown in Figure 5.27. The samples with 50, 100, 200, 500, and 800 mM of PTh clearly show the coating of PTh on each latex particle, which is shown in Figures 5.28-5.32. They also show no phase separation between the PTh and the NR. This suggests a high level of dispersability of rubber particles and PTh. The average particle diameter was estimated to be between 0.6-1.6 μm , or approximately the same as the value determined by the particle size analyzer. This also reveals the very fine nanometer thickness of the layer. As is

known, the morphology and electrical properties are the most importance relations for conductive polymers. The smooth surface of PTh-NR can be reason for the better conductivities ^[92]. Thus, a higher concentration of PTh can also enhance larger amounts of the irregular globular structure, this may leading to property improvement such as mechanical, and thermal properties and so on.

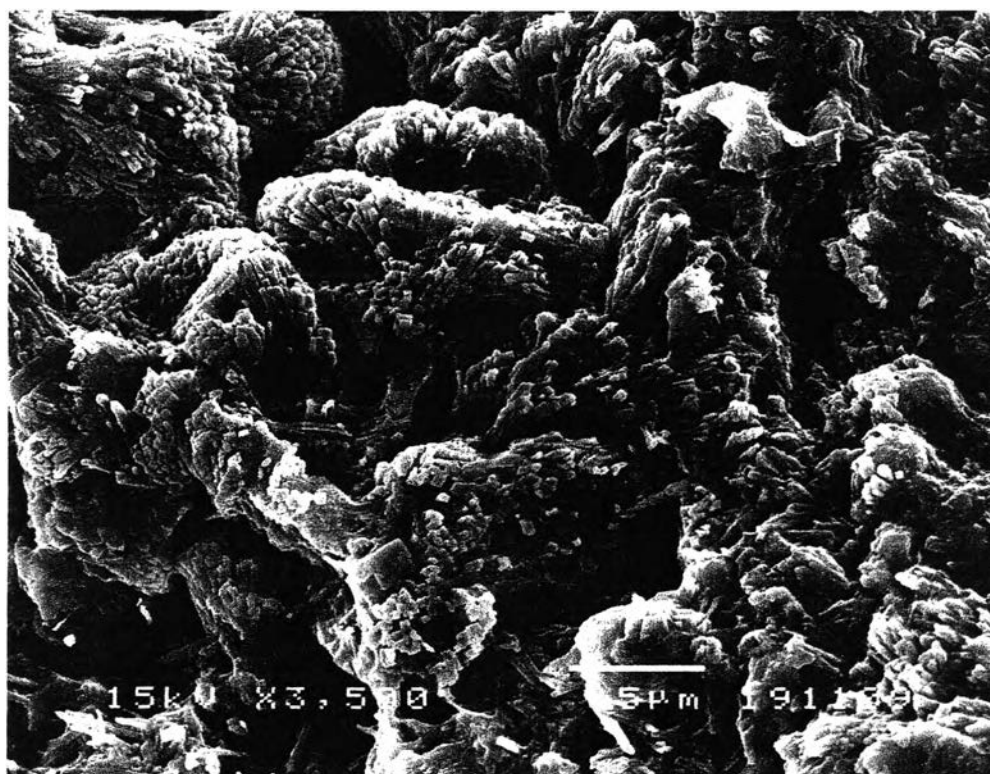


Figure 5.25 Scanning electron micrograph of the coat polythiophene by using electrochemical method; magnification 1,500/15 kV

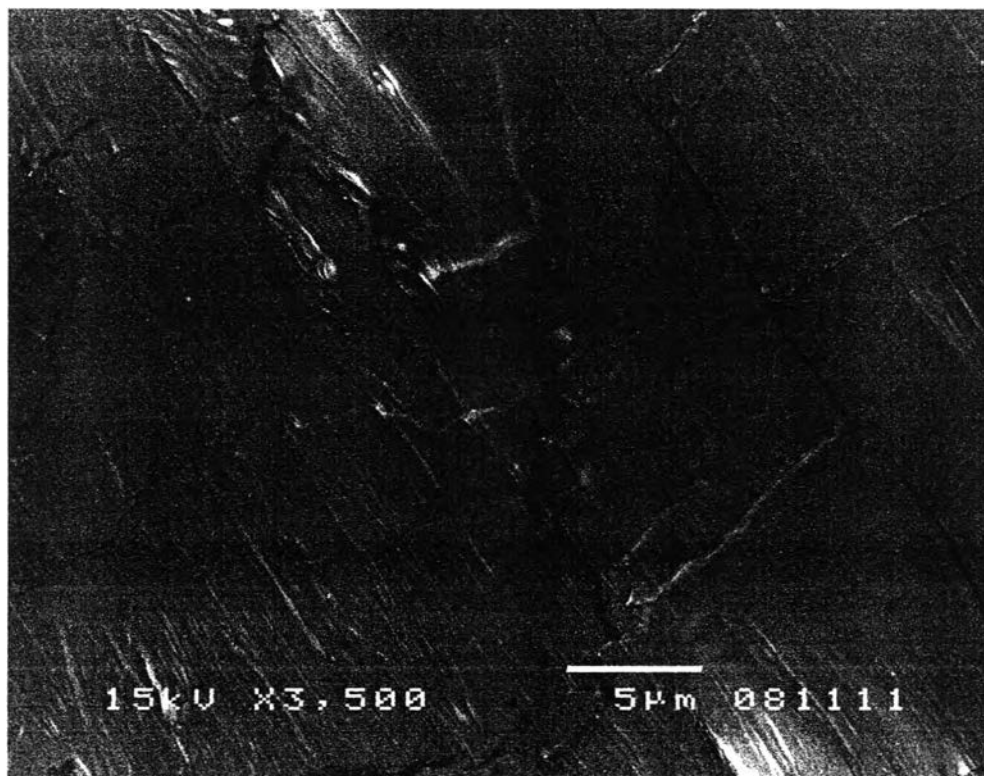


Figure 5.26 Scanning electron micrograph rubber magnification 1,500/15 kV



Figure 5.27 Scanning electron micrograph of the coated admicelled rubber (with 20 mM PTh) by using electrochemical method; magnification 1,500/15 kV.

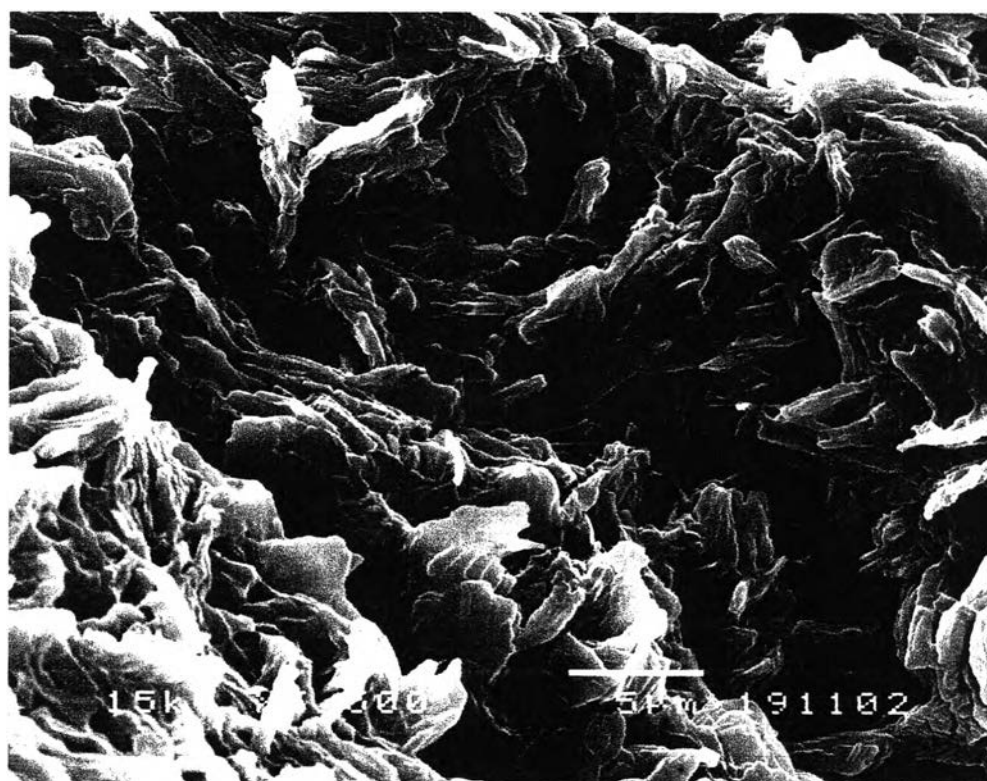


Figure 5.28 Scanning electron micrograph of the coated admicelled rubber (with 50 mM PTh) by using electrochemical method; magnification 1,500/15 kV

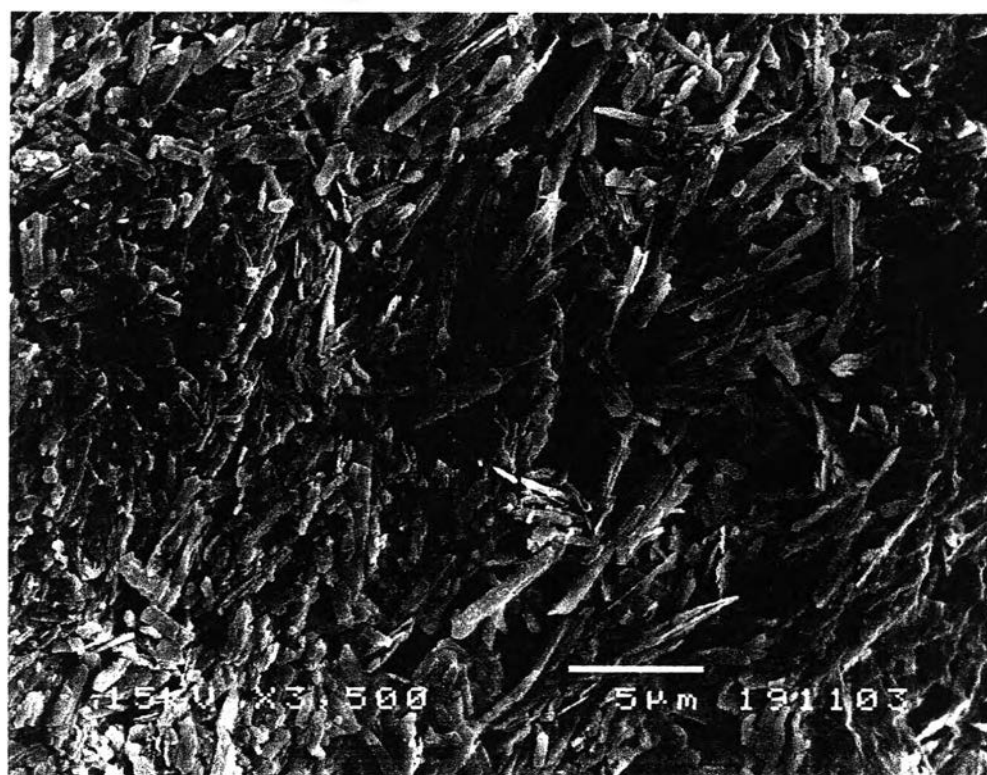


Figure 5.29 Scanning electron micrograph of the coated admicelled rubber (with 100 mM PTh) by using electrochemical method; magnification 1,500/15 kV



Figure 5.30 Scanning electron micrograph of the coated admicelled rubber (with 200 mM PTh) by using electrochemical method; magnification 1,500/15 kV

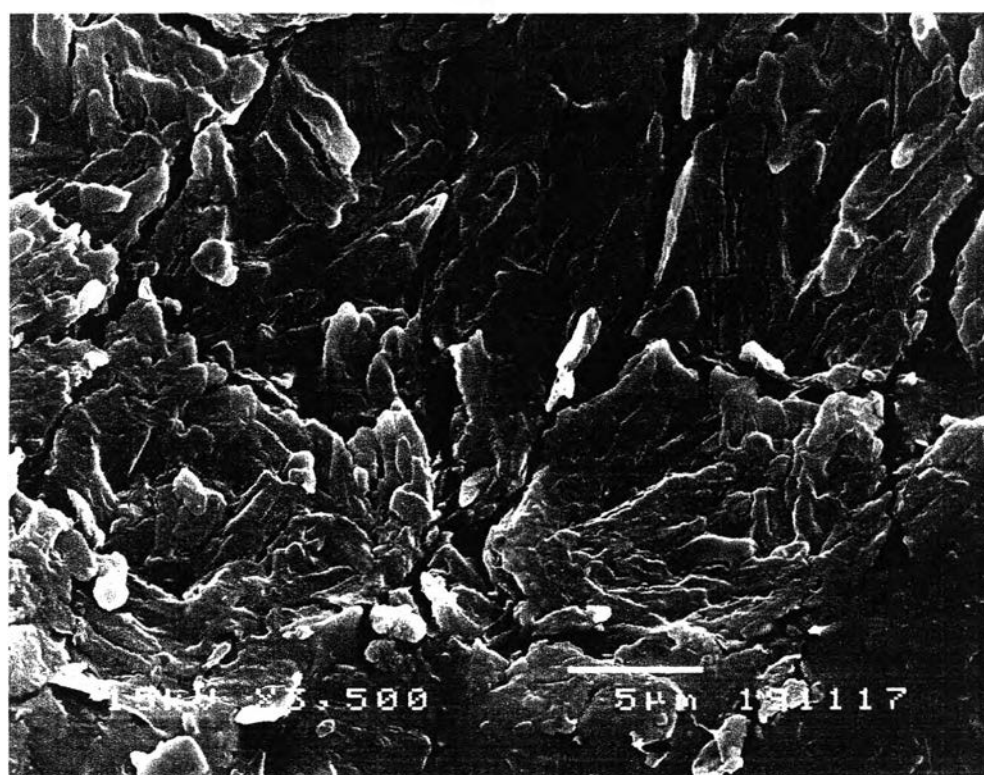


Figure 5.31 Scanning electron micrograph of the coated admicelled rubber (with 500 mM PTh) by using electrochemical method; magnification 1,500/15 kV

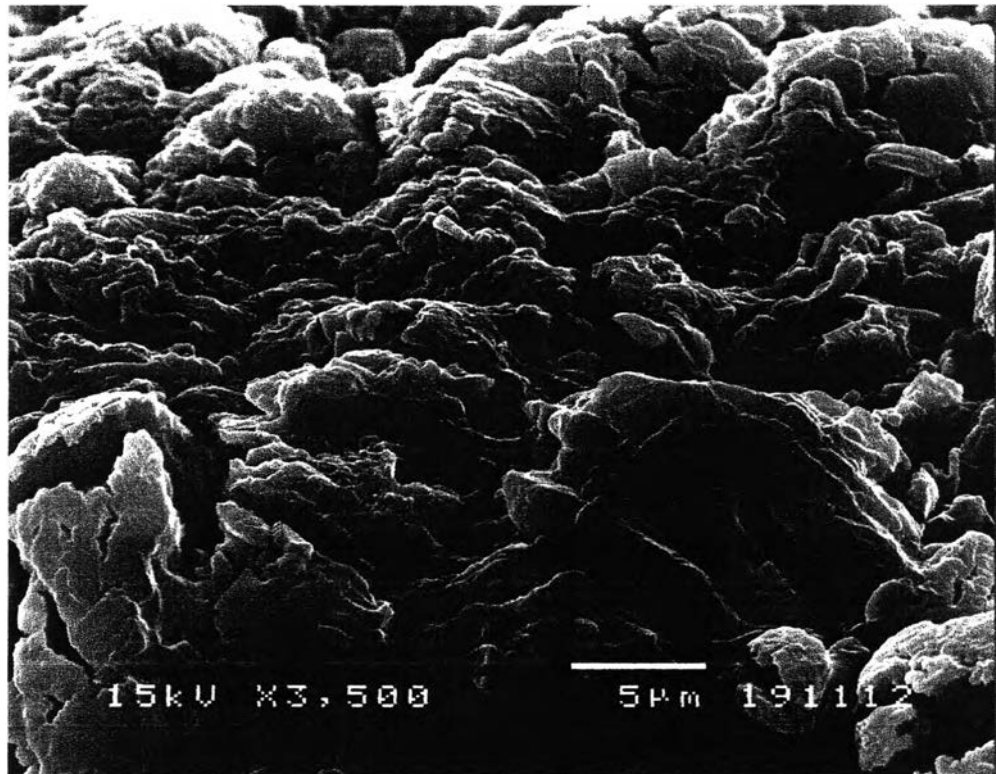


Figure 5.32 Scanning electron micrograph of the coated admicelled rubber (with 800 mM PTh) by using electrochemical method; magnification 1,500/15 kV

5.4.7 Thermogravimetric Analysis ^[92,100-101]

Thermal behavior of the samples was investigated by using a Thermogravimetric-Differential Thermal Analyzer (Perkin Elmer, Pyris Diamond) to study the thermal stability and decomposition temperature. TG-DTA patterns of the PTh-NR composites are shown in Figures 5.33-5.38 and in Table 5.9. It can be seen from the TGA curve that there is a 10% weight loss in the range of 100-250°C because of the evaporation of physically adsorbed water and loss of some surfactant and product surface. NR shows the major decomposition at 373.6°C and PTh starts to degrade the first step from 194.8°C, then shows the main mass loss at 211.4°C because of the rearrangement and degradation of the side chain (X. Hu et al., 2000)¹⁰¹. The second weight loss step, which took place in the temperature range of 438.6 to 899°C, corresponds to the degradation of the polymer backbone, leaving behind a residue content of less than 12.1%. Compared with result of M.Kabasakaloglu et al., (2001)¹⁰⁰, the highest decomposition temperature of PTh is 252°C whereas PT-DBSNa give the initial degradation temperature of 292°C, maximum degradation temperature is 671°C, and final degradation temperature is 908°C (A.Gok et al.,2007)⁹².

From the curve, the significant weight loss of the admicelled rubbers starts at around 347 to 350 °C (Figure 5.35). They lose more than 90% of their weight between 347 and 480°C. This suggests that the admicelled rubbers begin to lose weight at a higher temperature compared to that of NR and they also show the shift of major decomposition of pure PTh to higher temperature (T_d of rubber =373.6°C, T_d of PTh = 211.4°C, T_d of admicelled rubbers = 370.3 to 378.7°C). Compared with the results of M.Talu (2001)¹⁰⁰, the three decomposition temperatures (T_i , T_m , T_f) of the PF/PT bipolymer can be improved, where PTh has T_i =220°C, T_m =340°C, and T_f =465°C. This indicates better thermo stability of the admicelled rubbers caused by admicellar polymerization. The DTG a curve of the admicelled rubber follows the shape of the DTG curve of pure rubber during heating from 30 to 400 °C. The reason is that the main composition is NR (% wt of PTh added is about 1-57%, seen in Table A2), indicating that rubber is the dominate factor affecting the thermal stability of the admicelled rubbers. Moreover, this decomposition can attribute to the swollen NR that acts as binder between admicelled NR particles. The second decomposition goes on as a shoulder at high temperature 400-500 °C where about 40-50 %wt of admicelled

NR are now decomposed. Indeed, the peak temperatures (Figure 5.35) of the admicelled rubbers are higher than that of pure rubber (373.6°C). The higher the PTh content, the slower the samples start to degrade. This fact also supports the above mentioned results that coating PTh by admicellar polymerization improves the thermostability of NR.

The decomposition temperatures were also ended at higher temperature (597.46°C) than that of pure rubber (471.9 °C) as shown in the Table 5.9, higher ending temperature with higher PTh content (Figure 5.37). The higher the PTh content, the slower the samples start to degrade. This attribute to PTh coating that shields the core NR from early decomposition. This fact also supports that coating PTh encapsulating NR by admicellar polymerization can improve the thermostability of natural rubber

Moreover, the curves also demonstrate that char yields of the admicelled rubbers increased from 1% of pure rubber to 57.38% related to the content of PTh added. The residual content of samples with PTh 20 mM (4.9 %wt) are about 1%; PTh 50 mM (10.113%wt), 1.7%; PTh 100mM (18.69 %wt), 2.9%; PTh 200 mM (31.49 %wt), 3.2 %; PTh 500 mM (53.47 %wt), 3.4 %; and PTh 800 mM (64.77% wt), 3.9%. These indicate that an increase of PTh content enhanced the residue remaining (the residual content of pure PTh is 12.1%), Figure5.38.

Table 5.9 Degradation temperature of the admicelled rubbers

Sample	Onset Temperature	End point Temperature	Peak temperature	Residual content (%)
Rubber	351.6	471.9	373.6	1.1
20	347.6	473.5	370.3	1
50	348.3	475.1	372.1	1.7
100	348.5	476.3	374.5	2.9
200	348.4	476.6	374.8	3.2
500	348.6	478.9	375	3.4
800	350.8	480.9	378.7	3.9
PTH	343.1	597.4	375.3	17.3

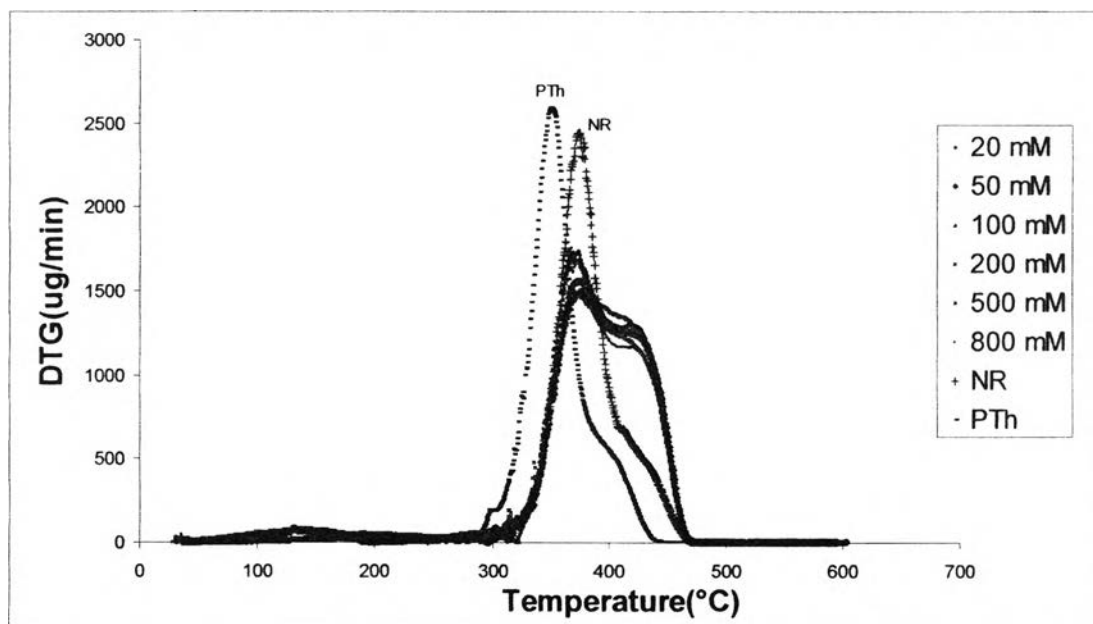


Figure 5.33 DTG thermograms at 10 °C/min nitrogen atmosphere of admicellar rubbers with SDS by using electrochemical methods.

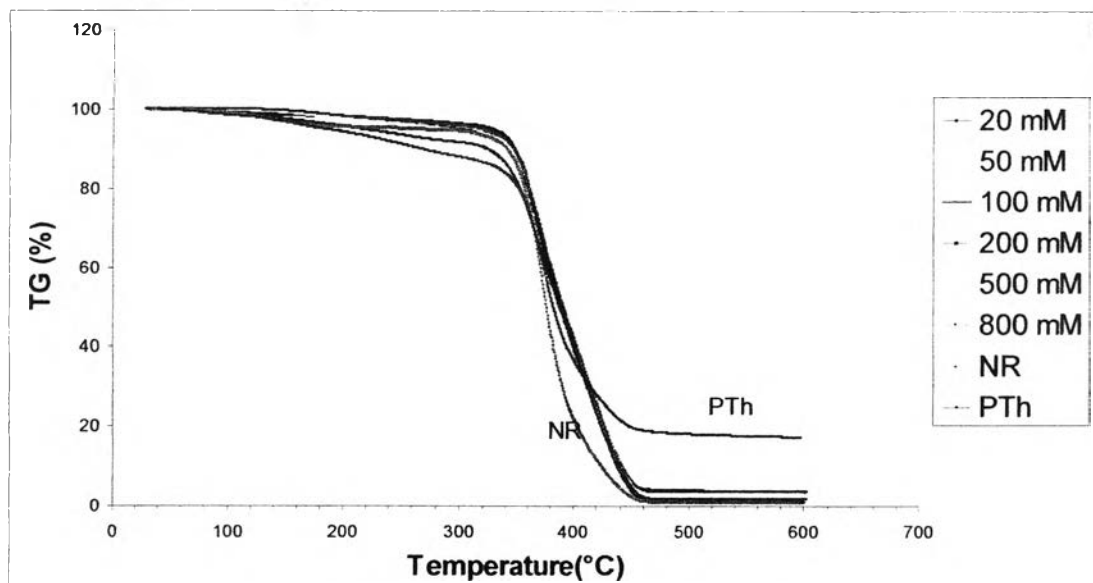


Figure 5.34 Thermogravimetric analysis thermograms at 10 °C/min in nitrogen atmosphere of admicellar rubbers with SDS by using electrochemical methods.

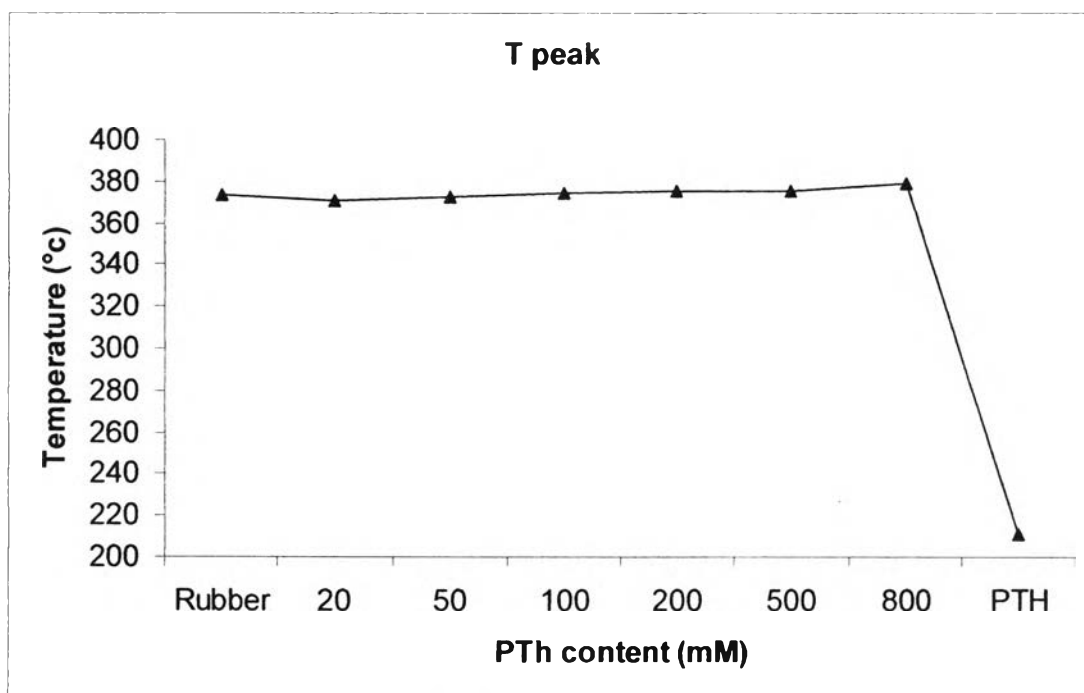


Figure 5.35 Thermogravimetric analysis thermograms at 10°C/min in nitrogen atmosphere of admicellar rubbers with SDS by using electrochemical methods.

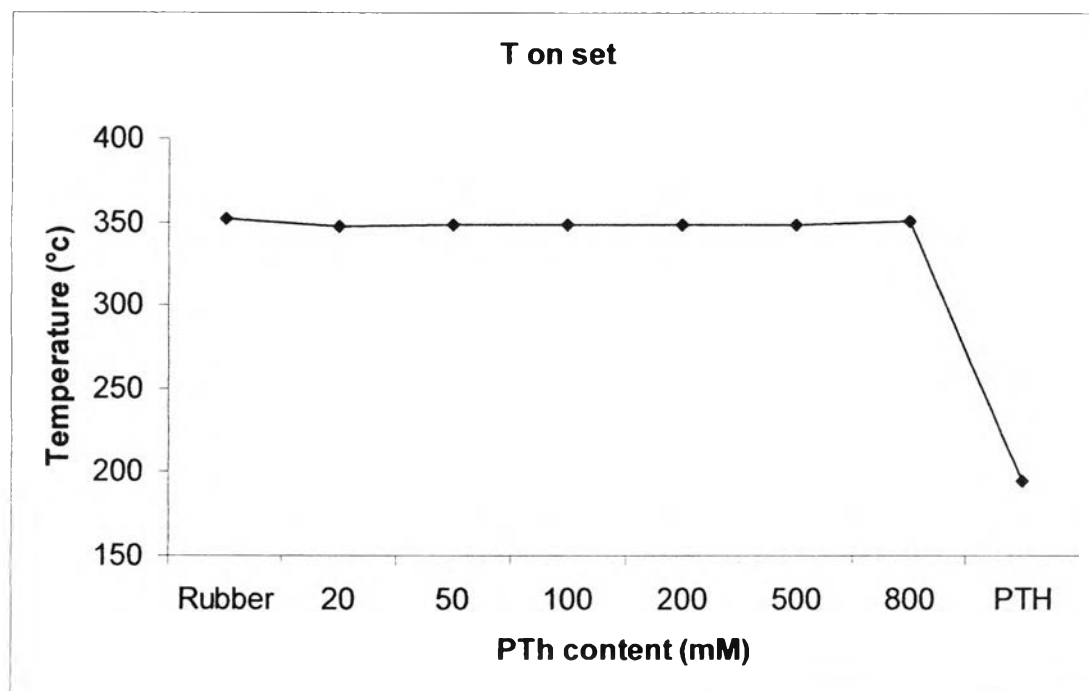


Figure 5.36 Thermogravimetric analysis thermograms at 10 °C/min in nitrogen atmosphere of admicellar rubbers with SDS by using electrochemical methods.

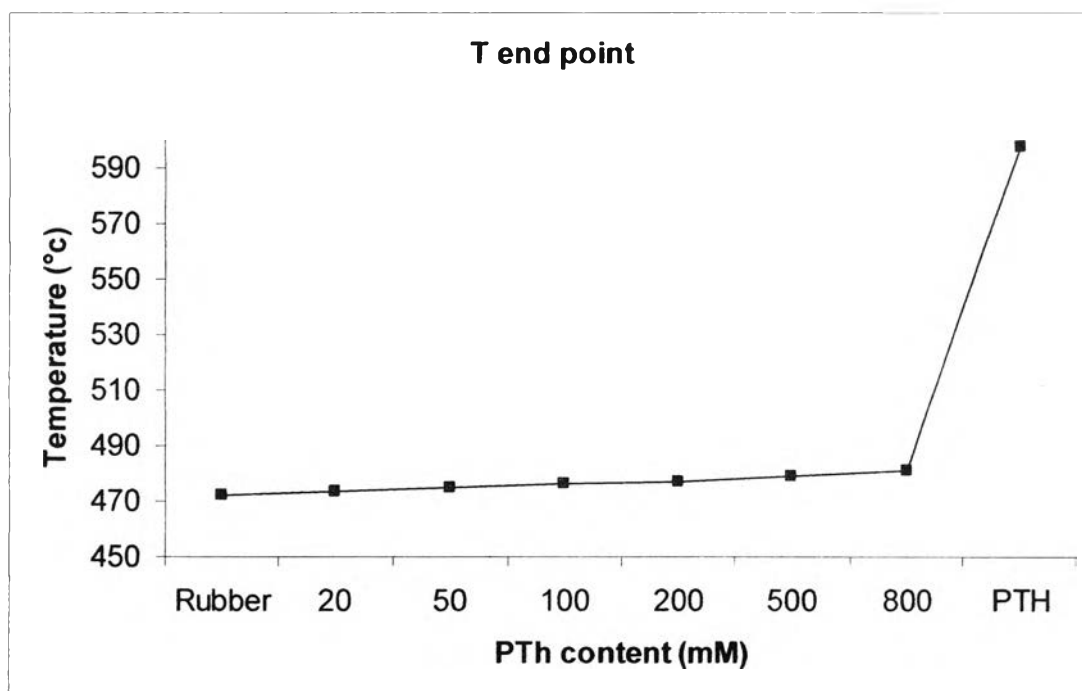


Figure 5.37 Thermogravimetric analysis thermograms at 10°C/min in nitrogen atmosphere of admicellar rubbers with SDS by using electrochemical methods.

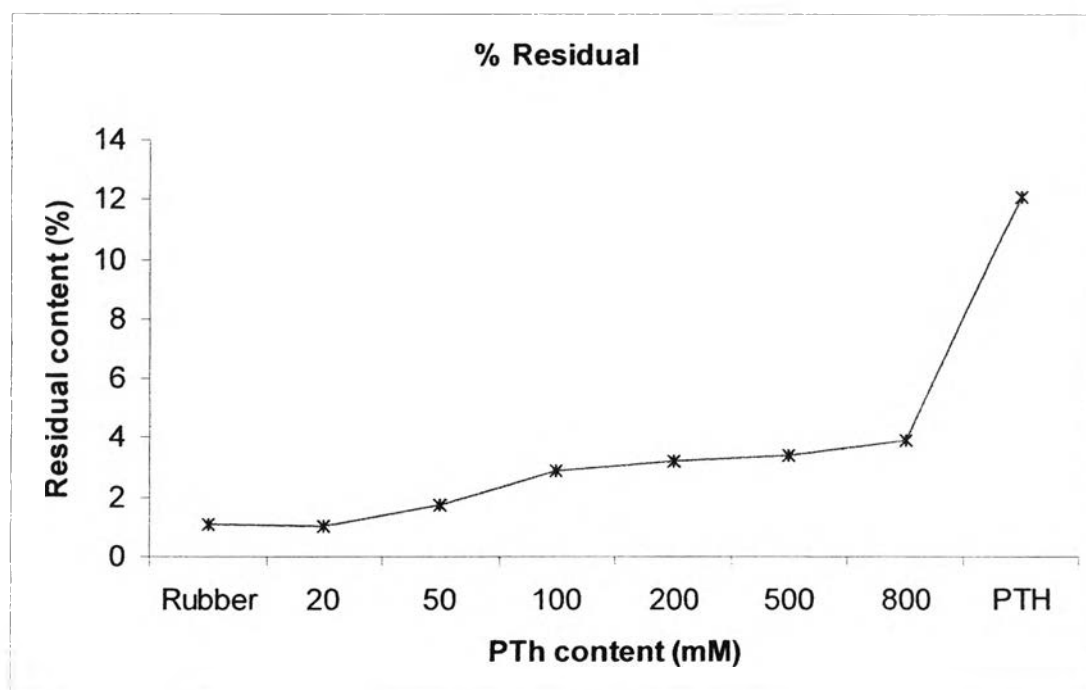


Figure 5.38 Thermogravimetric analysis thermograms at 10°C/min in nitrogen atmosphere of admicellar rubbers with SDS by using electrochemical methods.

5.4.8 Mechanical Properties Measurement

5.4.8.1 Lloyd Universal Testing Machine^[112-116]

The mechanical properties of the admicelled latex films were determined using a Lloyd Universal Testing Machine with a crosshead speed of 50 mm/min, and gauge length of 50 mm, under room temperature. The tests followed ASTM D882-91. The effects of thiophene concentration on the mechanical properties of admicelled rubber films are shown in Figures 5.39-5.42. Table 5.10 shows that the pure NR film was soft, tough, and highly elastic, with high elongation at break (311.75 %), a high value for work to break (0.672 J), but low tensile strength at break (4.8657×10^5 Pa) and low young's modulus (0.167 MPa). Since Polythiophene is insoluble, infusible, brittle and hence unprocessable. The admicelled technique with electrochemical polymerization was developed to increase its processability which changes from soft and elastic to hard and stiffness. Increasing the concentration of PTh into Natural rubber indicates that stiffness and strength was affected. The tensile strength at break can be improved from $2.036 \pm 0.283 \times 10^5$ Pa to $13.385 \pm 0.898 \times 10^5$ Pa (Figure 5.40).

The mechanical properties are unsatisfactory at low composition, it can explain by SEM results. At small amount of PTh, it clearly seen that there are few voids, porous structure and more agglomerated grains as a rigid rod like overlap each other. These microstructures lead to their strengths per unit thickness become weaker at lower amount of PTh (Xi-Shu.W et al. 2002)¹¹⁵. Therefore, the higher amount of monomer content can results in the higher in tensile strength due to monomer are tightly contact and becomes continued matrix. The maximum tensile strength was 4 time higher than that of natural rubber. This values is still lower than the results of Y.Sun et al.(1995)¹¹⁶ that tensile strength of poly(3-methylthiophene) on rubber (SBS) increases from 7.9-29.2%wt, the tensile strength become increasingly from 10 to 14.3 Mpa. The reasons are the different in their molecular structure poly(3-methylthiophene) as monomer, it consist of introduced a long (number of carbon atoms in the chain was at least four) alkyl, alkoxy, alkylsulfonate group in the 3-position of thiophene to generate soluble polythiophene derivertives ; the second was based on processable copolymers such as polythiophene-poly(vinyl alcohol) graft polymer ; the third was based on composites with polythiophene or its insoluble de-

rivative as a conductive component and another polymer as the polymer as the flexible one. However, the elongation at break decrease from 313 to 69.60 %.(Figure5.41) It was confirmed the similar trends by work to the break values (Figure5.42) from 0.55 to 0.24 J. This result is higher than that of Y.Sun et al.(1995)¹¹⁶ the elongation of PMT-SBS (from 7.9-29.2%wt) become decreasingly from 310 to 42 %. Furthermore, the young's modulus is built up from 1.1-2.85 MPa with increasing PTh content revealing the higher in their stiffness as shown in Figure 5.43.

Indeed, the admicelled technique can improve their mechanical properties and processability. The higher PTh content in the admicelle rubber, the lower elongation at break is and the higher tensile strength at break can improve.

Table 5.10 Composition and properties of PTh/NR were obtain by admicellar technique with UTM (Lloyd universal machine)

Sample (mM)	Elongation at break (%)	Tensile strength at break (MPa)	Work to Break (J)	Young's modulus (MPa)
NR	311.75 ± 6.23	0.48657 ± 0.002	0.6724 ± 0.013	0.1667± 0.013
20 (B2)	312.73 ± 15.378	0.2036 ± 0.0283	0.746 ± 0.0402	0.2857± 0.006
50 (B5)	198.80 ± 9.141	0.2952 ± 0.0501	0.561 ± 0.0678	0.4000± 0.008
100 (B10)	139.34 ± 8.512	0.2501 ± 0.02501	0.269 ± 0.0301	0.5714± 0.011
200 (B20)	129.01 ± 13.113	0.2963 ± 0.0338	0.249 ± 0.0237	0.5142± 0.010
500 (B50)	83.77 ± 14.896	0.9661 ± 0.0749	0.244 ± 0.0091	1.710± 0.034
800 (B80)	69.60 ± 5.143	1.3385 ± 0.0898	0.236 ± 0.0205	2.850± 0.057

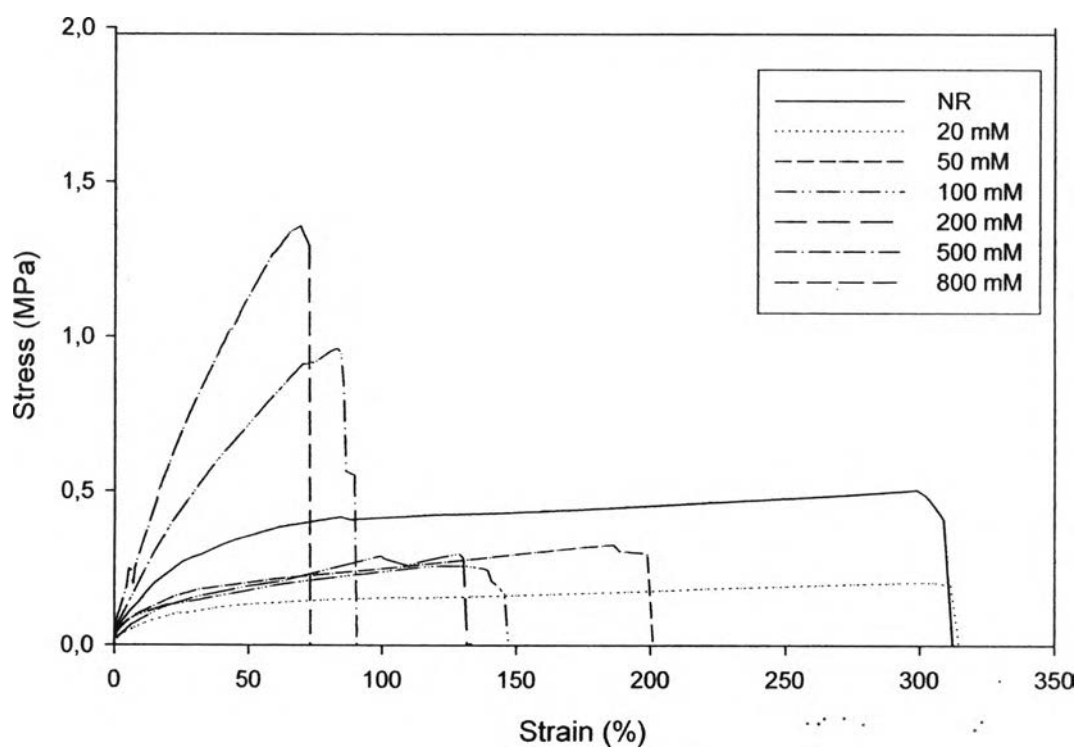


Figure 5.39 Effect of polythiophene concentration on the stress-strain curves of admicelled rubber

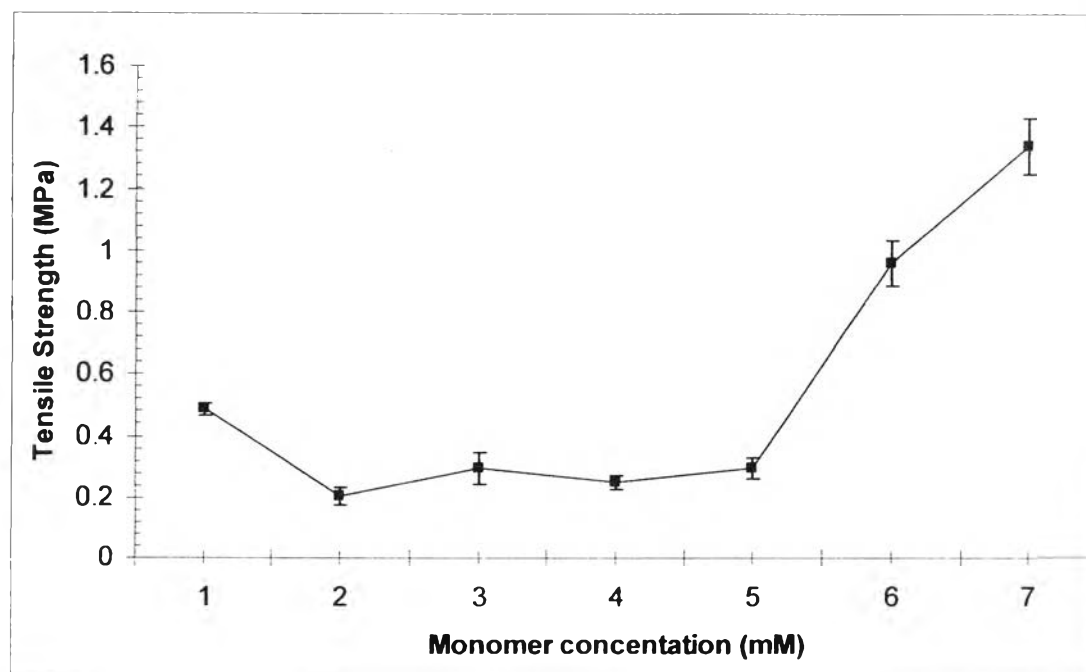


Figure 5.40 Tensile strength vary the concentration of polythiophene (Lloyd universal machine)

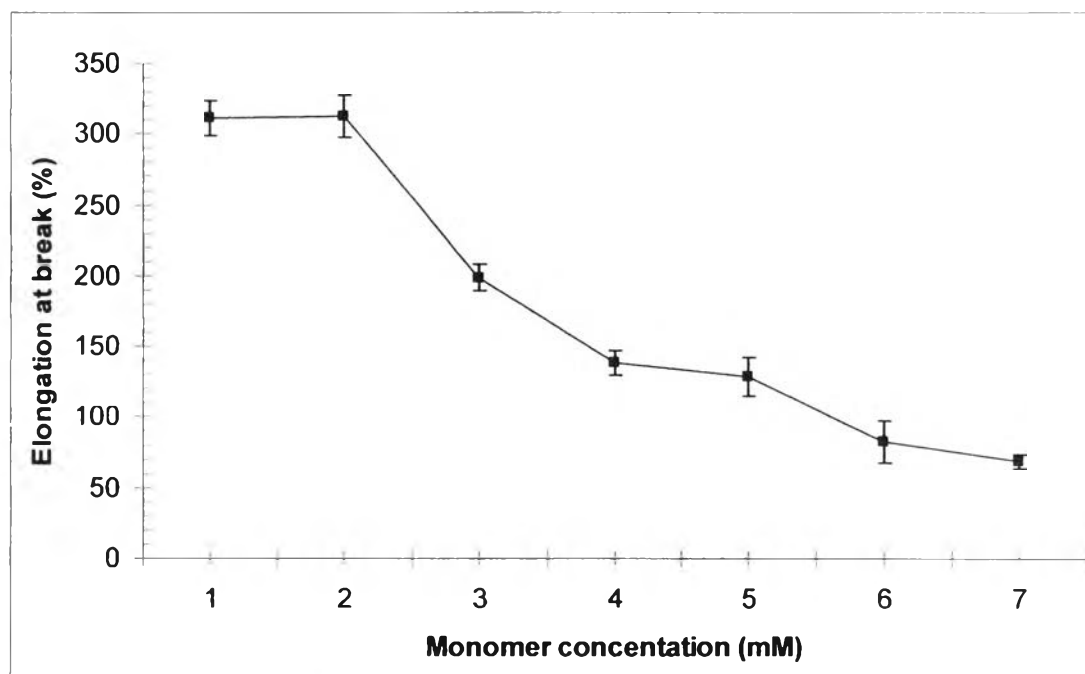


Figure 5.41 Elongation vary the concentration of polythiophene (Lloyd universal machine)

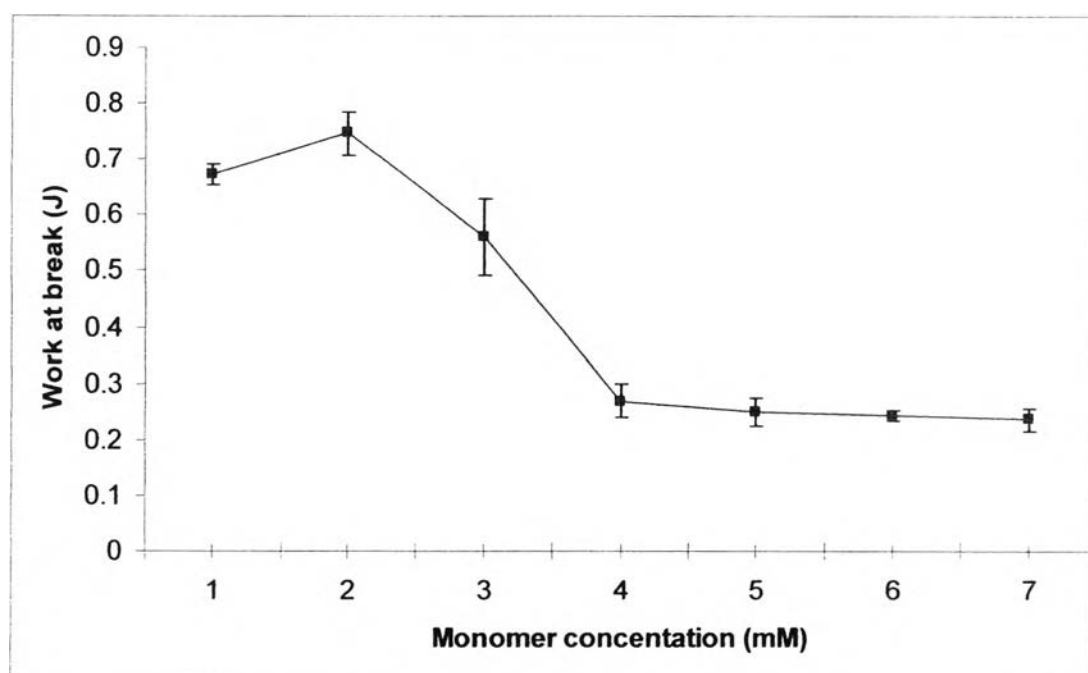


Figure 5.42 Effect of polythiophene concentration to work at break (Lloyd universal machine)

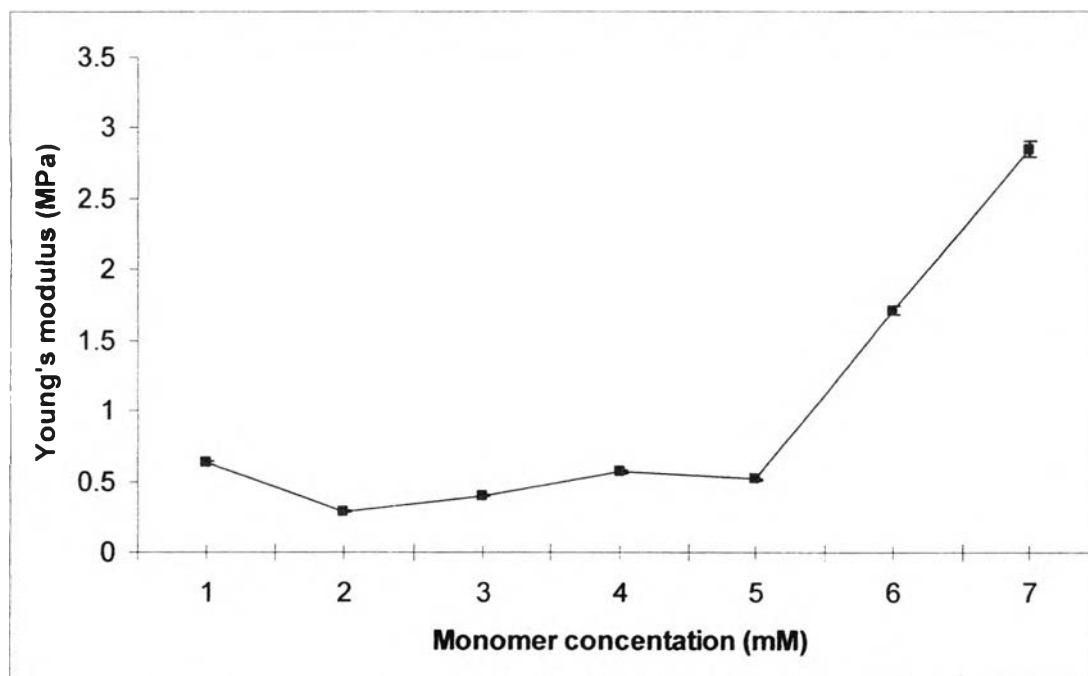


Figure 5.43 Effect of polythiophene concentration to Young's modulus (Lloyd universal machine)

5.4.8.2 Instron Universal Testing Machine

The mechanical properties were confirmed by using instron UTM testing with crosshead speed 50 mm/min gauge length of 13 mm, and load cell 100 kN under room temperature and the test was repeated 5 times. The dumbbell shape, which has thickness larger than 3 mm, was cut by using the pneumatic punch following ASTM D638M-91a. The tensile tests show higher stiffness of the admicelled rubbers than that of natural rubber (Figure 5.44-5.48). The elongation at break of NR is about 831 % while those of the admicelled rubbers are around 302.31-664.28% (Table 5.11 and Figure 5.46); increasing PTh content shows more brittleness (reducing Elongation) due to the rigidity of PTh. This study is correlated with Ruckenstein E. et al. (1995)¹¹⁶ reports. Tensile strength of uncrosslinked natural rubbers (thickness around 3 mm) is close to 1.5 MPa and tensile strength of the admicelled rubbers are around 1.1-11.61 MPa (Figure 5.45). The maximum tensile strength of the admicelled rubbers is 11.61 MPa which is higher than the testing by using the Lloyd Universal Testing Machine because of different in their thickness and size. It could be confirmed by Demirhan .E et al.(2006)¹¹⁸ which studied the physical properties of vulcanized SBR-1712 with adding carbon black content such as tensile strength is around 5-14 MPa. The results showed the similar trends which rubber reduces stiffness of conductive composite and it results in such a reasonable tensile strength. The work to the break results also shows the brittleness of admicelled NR developed by with increasing PTh content. It decreased from 0.38 to 0.28 J as higher amount of polythiophene (Figure 5.47). Young modulus increased from 0.3 MPa (NR) to 5.4 MPa at 800 mM showing the increase in stiffness of the admicelled NR with PTh content (Figure 5.48).

Table 5.11 Composition and properties of PTh/NR were obtained by admicellar technique with UTM (Instron Machine)

Sample (mM)	Elongation at break (%)	Tensile strength at break (MPa)	Work to Break (J)	Young's modulus (MPa)
NR	831.46 ± 16.63	1.3011 ± 0.026	1.0181 ± 0.020	0.333 ± 0.006
20 (B2)	664.28 ± 33.21	1.1041 ± 0.171	0.3861 ± 0.029	0.166 ± 0.003
50 (B5)	567.57 ± 31.87	2.9181 ± 0.212	0.3920 ± 0.110	0.333 ± 0.006
100 (B10)	431.31 ± 29.23	2.9113 ± 0.218	0.3645 ± 0.058	0.370 ± 0.007
200 (B20)	420.86 ± 21.78	5.8101 ± 0.125	0.3123 ± 0.027	0.833 ± 0.016
500 (B50)	375.08 ± 18.10	8.7012 ± 0.141	0.2901 ± 0.049	1.176 ± 0.023
800 (B80)	302.31 ± 16.11	11.6101 ± 0.179	0.2817 ± 0.012	5.405 ± 0.108

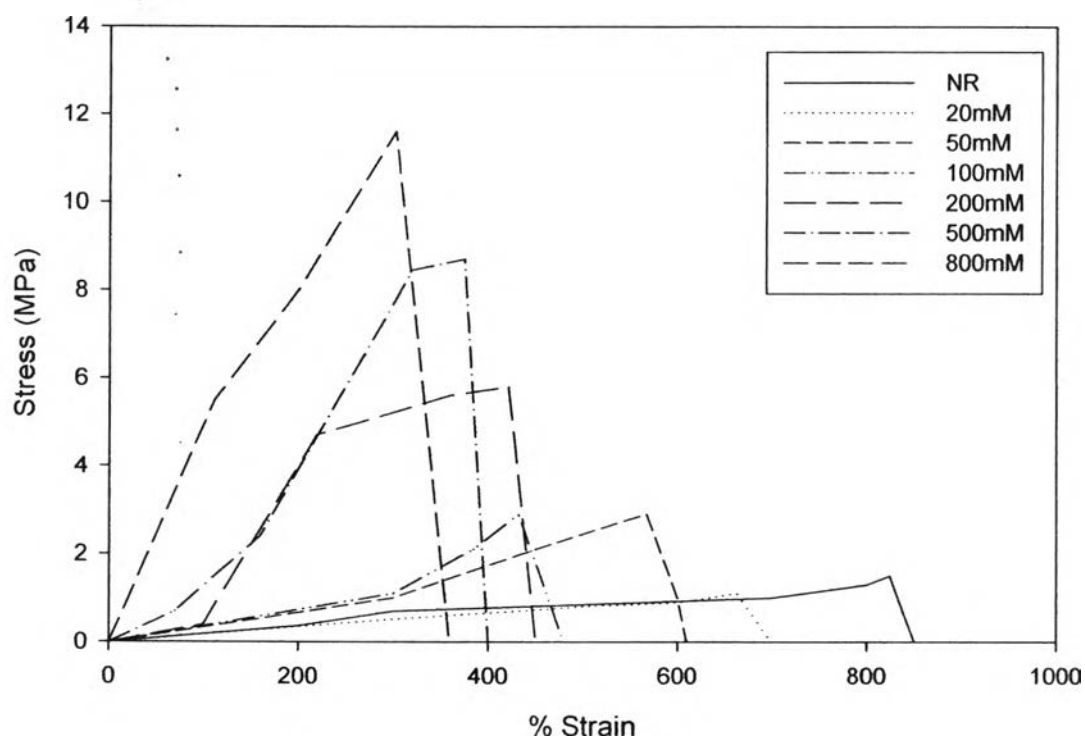


Figure 5.44 Effect of polythiophene concentration on the stress-strain curves of admicelled rubber.

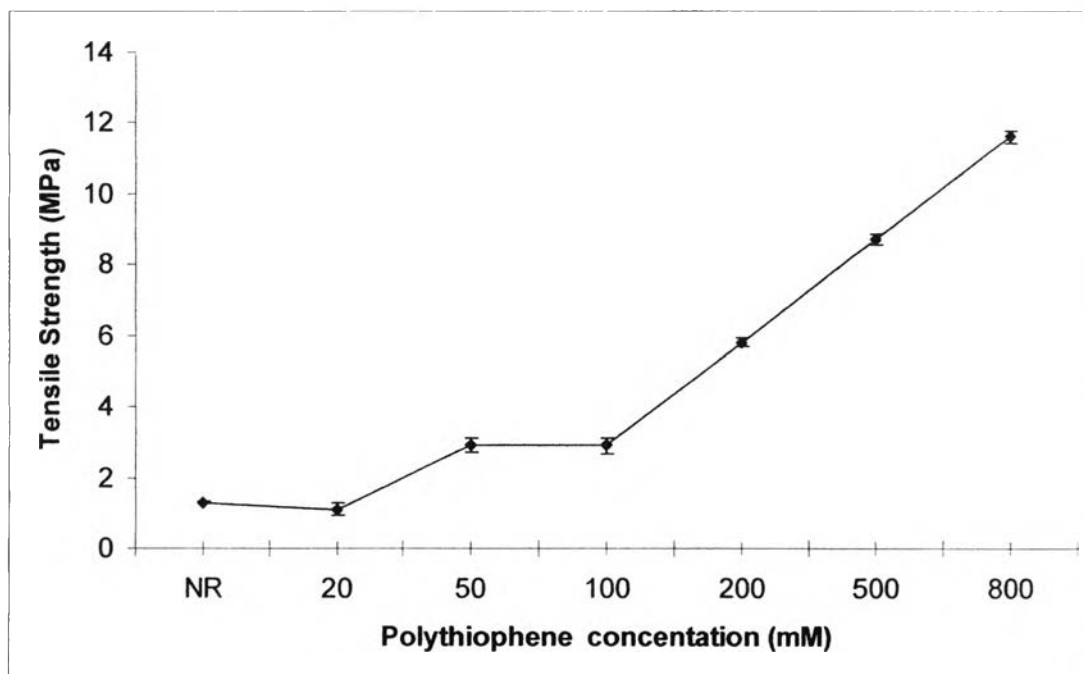


Figure 5.45 Tensile strength vary the concentration of polythiophene (Instron machine)

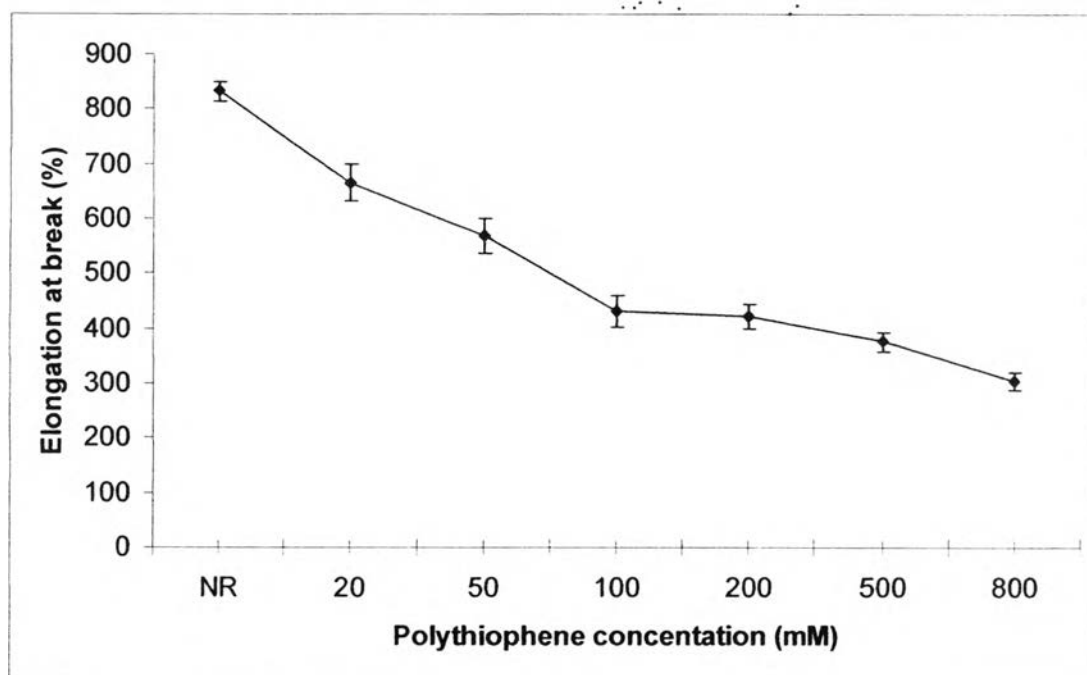


Figure 5.46 Elongation vary the concentration of polythiophene (Instron machine)

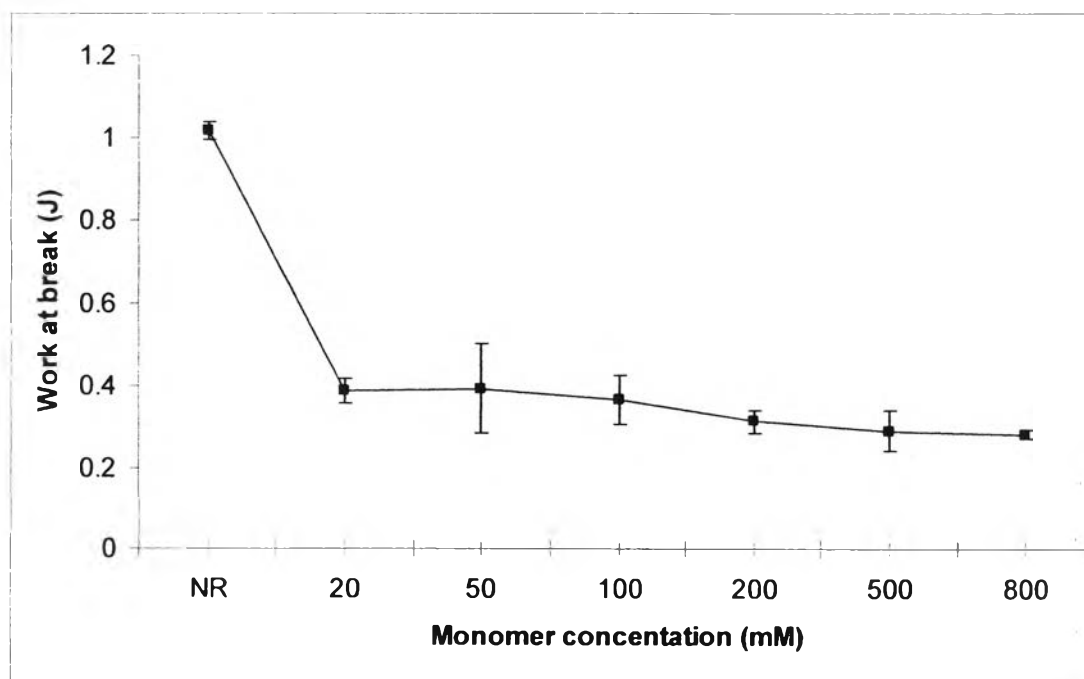


Figure 5.47 Effect of polythiophene concentration to the energy at break.

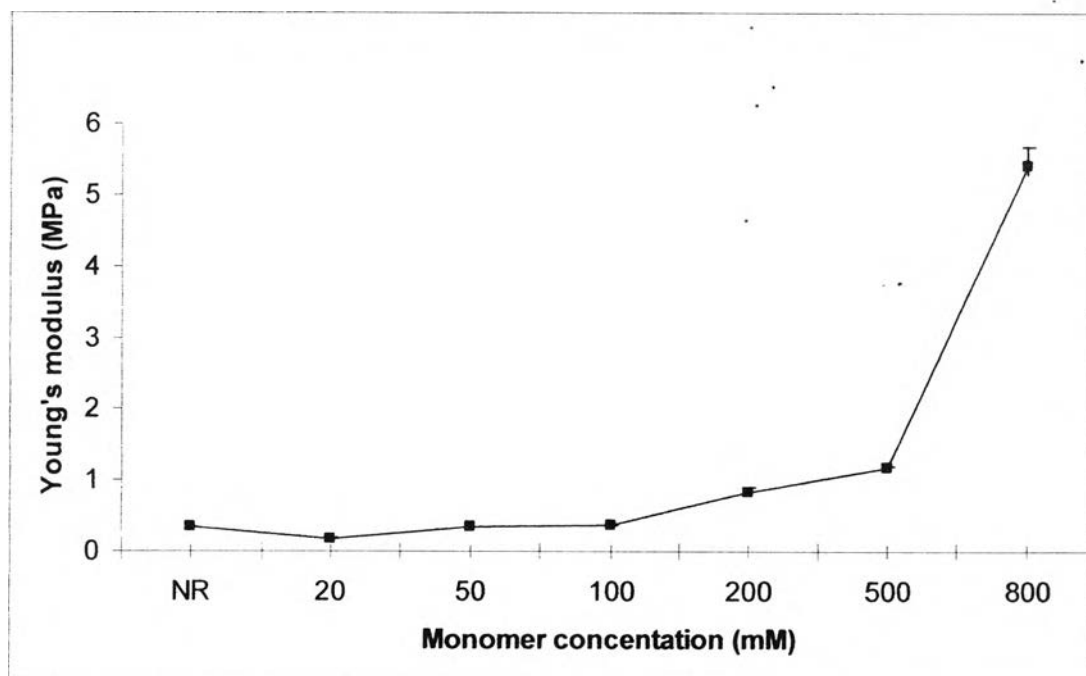


Figure 5.48 Effect of polythiophene concentration to Young's modulus.

5.4.9 ShoreA and ShoreD Hardness Measurement ^[119-121]

The shore A and D hardness values for the samples are presented in Table 5.12, which follow the ASTM D2240 , ISO868 , DIN 54505, BS 2782 Method 365 B. The variation of hardness of the samples is similar to tensile strength as shown in the Figures 5.49-5.50. In general, the elongation of admicelled rubber decreases whereas the hardness of that increases. From Table 5.12, the hardness of natural rubber is 22.46 and admicelled rubbers are increased from 18.28 shore A up to 88.6 shore A. The hardness was abruptly developed at about 500 mM PTh content corresponding to the dense packing of PTh particles. The admicelled NR become hard like plastics. The hardness was also measured by hardness shore D which increased from less than 10 to 16.9 shore D. The hardness of admicellar rubber corresponded to the concentration of conductive polymer which has higher hardness because of good interfacial adhesion between the matrix and the dispersed phase (S. Lopez, 2004)¹¹⁹. Therefore, hardness can be increased with the conductive polymer loading in the composite (Demirham, 2006)¹¹⁸. These are strong evidence to improve their hardness properties.

Table 5.12 Shore hardness with concentration for admicellar rubber^{18,19,20}

Polythiophene concentration (mM)	Hardness (ShoreA)	Hardness (ShoreD)
NR	22.46154	<10
20	18.28571	<10
50	25.28571	<10
100	26.85714	<10
200	36.28571	<10
500	66.5	13.2
800	88.66667	16.9

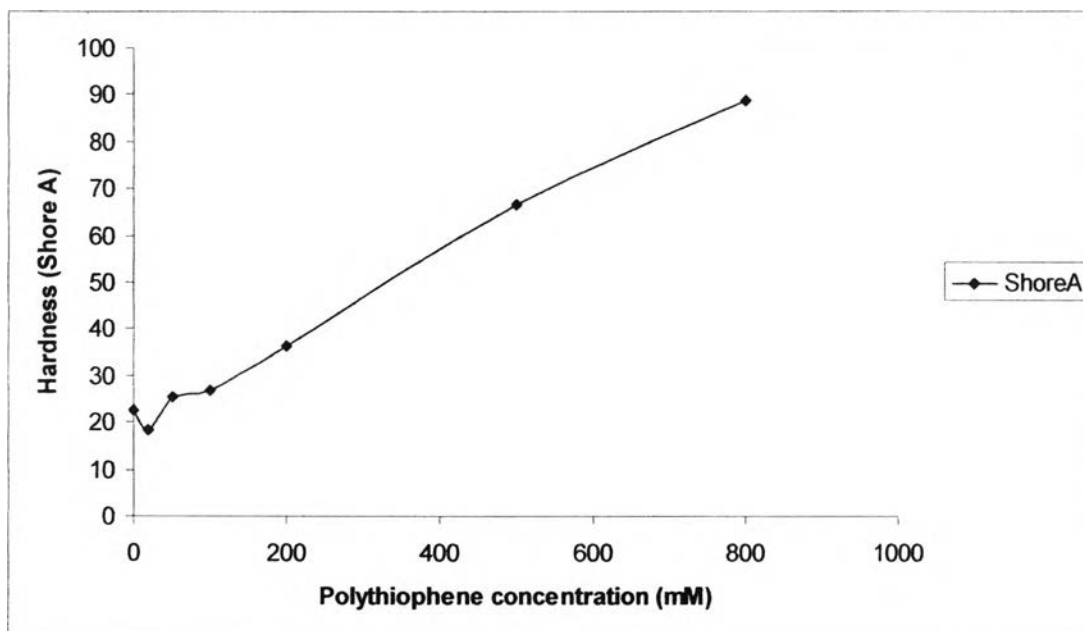


Figure 5.49 Variation of hardness shoreA with polythiophene concentration for admicellar rubber

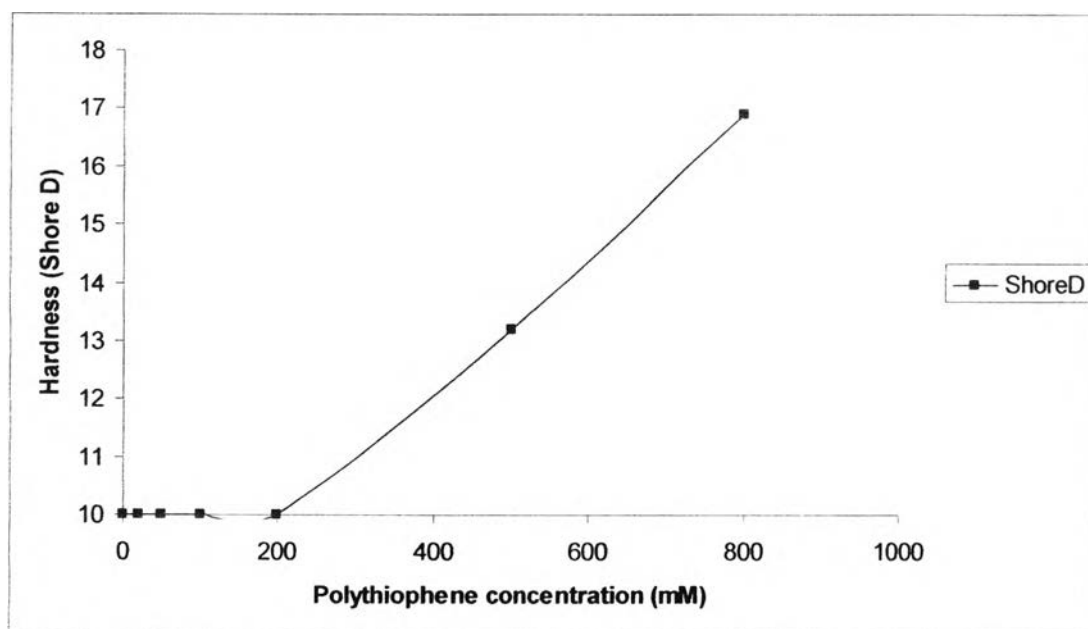


Figure 5.50 Variation of hardness shoreD with polythiophene concentration for admicellar rubber

5.4.10 Conductivity Properties Measurement

The conductivity of admicellar rubber were tested by using Keithley 8009 Resistivity Test Fixture and Keithley 6517A Electrometer/ High Resistance Meter. The dc voltage from 1 to 15 volts was applied to the specimen, placed in the Keithley 8009 Test Fixture.

After the current was read, the surface and the volume resistivities were determined as shown in Tables 5.13-5.14. Figure 5.51 shows the effect of thiophene monomer content on the electrical conductivity admicelled PTh/rubber. In Figure 5.52, the percolation threshold of PTh in the admicelled PTh/NR products is found at volume fraction of 0.16 that raise the electrical conductivity to 2.86×10^{-8} S/cm, several orders from the insulator NR (10^{-15} S/cm). Then the conductivity increases gradually with PTh content and increasing significantly at 500-800 mM thiophene or volume fraction of 0.49-0.60 corresponding to the change in denser and smoother admicelled PTh/NR morphology (Y.A. Adum et al. 2005 [29]). The electrical conductivity as high as 8.26×10^{-6} S/cm could be finally obtained. The thiophene promotes an increase of nine orders of magnitude on the conductivity of NR, ranging from 10^{-15} to 10^{-6} S/cm. Other work by Semih.Y et al.(1996,[28]) reported that 80%wt PTh-NR made by electrochemical polymerization of thiophene onto rubbers had conductivity in the range of $2.6-3.5 \times 10^{-1}$ S/cm depending on doping condition.

Table 5.13 Conductivity of natural rubber sheet at various PTh content

PTh (mM)	PTh : NR %	Resistivity V $\Omega \cdot \text{cm}$	σ_v $\text{S} \cdot \text{cm}^{-1}$	Resistivity S Ω	σ_s S	Thickness (cm)
Rubber	-	1.39E+14	7.18E-15	4.07E+14	2.46E-15	0.334
20	4.3935	3.97E+11	2.52E-12	5.40E+11	1.85E-12	0.387
50	10.3113	3.88E+09	2.57E-10	7.08E+10	1.41E-11	0.394
100	18.6913	3.50E+07	2.86E-08	7.61E+07	1.31E-08	0.395
200	31.4957	1.12E+07	8.94E-08	7.13E+07	1.40E-08	0.391
500	53.4755	1.87E+06	5.35E-07	3.61E+06	2.77E-07	0.490
800	64.7769	1.21E+05	8.26E-06	3.84E+05	2.61E-06	0.413
PTh	100	7.17E+01	1.39E+00	7.56E+00	1.32E-01	0.0022

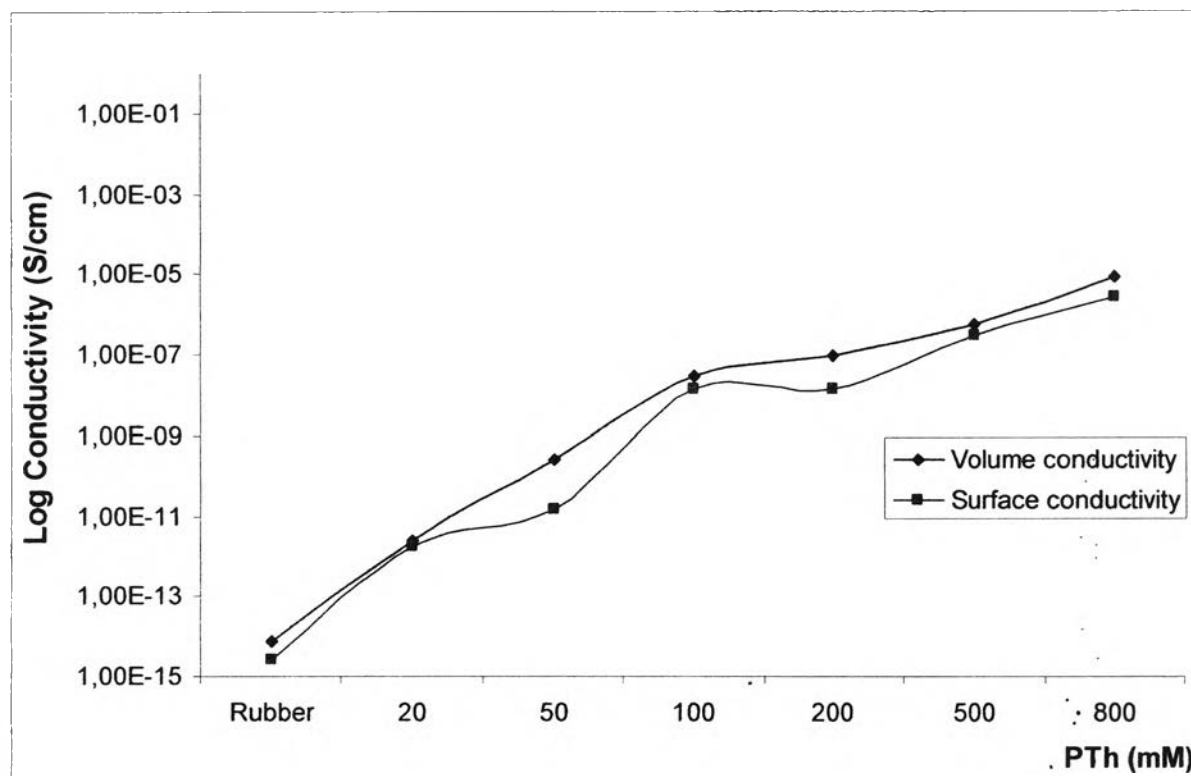


Figure 5.51 Electrical conductivity as a function of polythiophene content in composites with natural rubber latex (Apply dc 0.1-20 volt).

The increasing conductivity can be increased with amount of PTh. However, the conductivity is also depending on surfactant. From Gok.A et al. (2007)⁹² compare the composition and properties of PTh prepared in the presence of a surfactant: PT-DBSNa(5.1×10^{-5} S/cm), PT-TTAB(8.4×10^{-5} S/cm), PT-Tween20(4.6×10^{-5} S/cm) and without surfactant(1.7×10^{-5} S/cm). These results indicate that part of anionic surfactant can be incorporated into PT structure like the oxidant anion and acts as co-dopant. While, PT-Tween20 is used the very long aliphatic chain of surfactant can be a steric barrier to oligomerization of the thiophene radical-cations and later for the creation of PT chain. Polymerization of thiophene proceeds via radical-cation intermediates sensitive to the reaction environment. Therefore, the anionic surfactant (DBSNa) can favor thiophene radical-cation formation and can accelerate polymerization. On the other hand, the cationic surfactant (TTAB) disfavors of the production of thiophene radical-cation and slow polymerization.

Since the surfactant can give SO_3^- group, it can also be presents as counter ion in the positive charge self-doped copolymer. As the evident from increasing

number of thiophene units are incorporated in the polymeric structure, it can see that the higher conductivity values (Y.A udum et al. 2005)⁹⁶.

Table 5.14 Conductivity of natural rubber sheet prepared at 25°C, 9V, at various to volume fraction

Sample (mM)	$\phi_{NR} = \frac{V_{NR}}{V_{NR} + V_{PTh}}$	$\phi_{PTh} = \frac{V_{PTh}}{V_{NR} + V_{PTh}}$	σ_v S.cm ⁻¹	σ_s S
Rubber	1	0	7.18E-15	2.46E-15
20	0.9669	0.0331	2.52E-12	1.85E-12
50	0.9208	0.0792	2.57E-10	1.41E-11
100	0.8536	0.1464	2.86E-08	1.31E-08
200	0.7442	0.2558	8.94E-08	1.40E-08
500	0.5379	0.4621	5.35E-07	2.77E-07
800	0.4211	0.5789	8.26E-06	2.61E-06
PTh	0	1	1.39E+00	1.32E-01

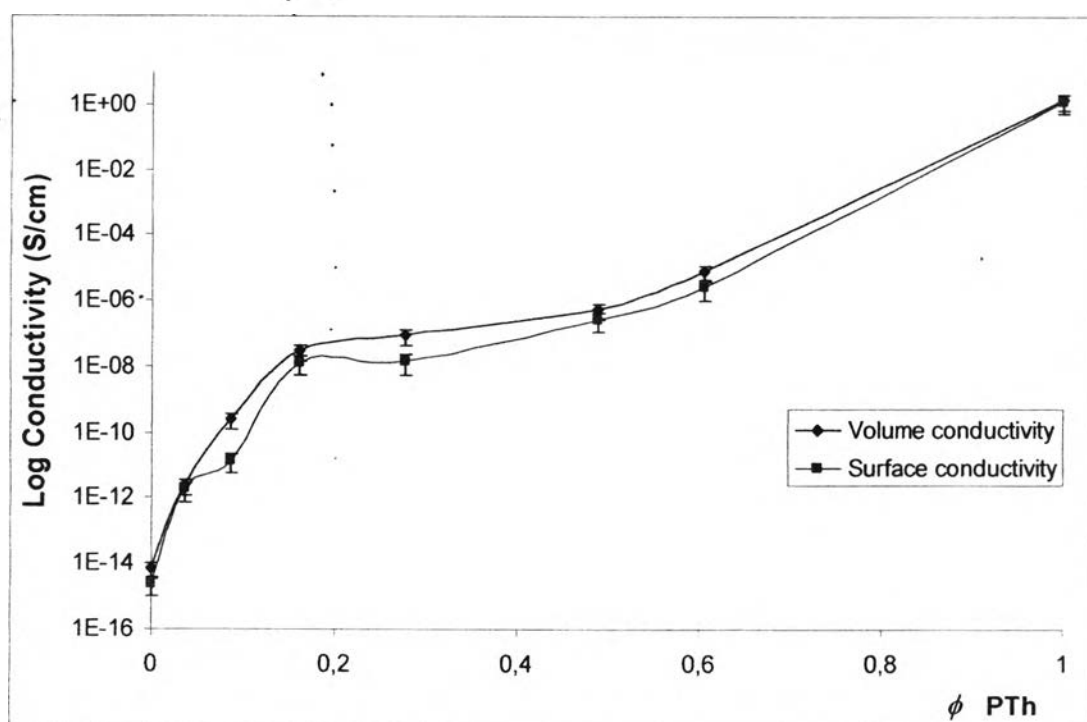


Figure 5.52 Percolation threshold of electrical conductivity as a function of polythiophene content in composites with natural rubber latex (applied dc 0.1-100 volts).

5.5 Conclusion

The success of the admicellar polymerization of polythiophene-coated latex particles was investigated using FTIR, SEM, TEM, and TGA. From the FTIR study, the admicelled rubbers showed the characteristic peaks of polythiophene, which confirmed the existence of PTh after the polymerization. The TEM and SEM micrographs revealed the even coating of PTh over latex particles and they showed the core-shell structure of PTh and NR. It also confirmed the faster polymerization at higher amounts of thiophene. This technique is efficient: % yield ~83-92%. As seen in the result of TGA, the admicelled rubbers began to lose weight at higher temperature, compared to that of NR, and they also showed the shift of major decomposition of pure PTh to higher temperature. The DTG curves also demonstrated an increase of char yields of the admicelled rubbers. As PTh content increased, the residual content also increased. This resulted in slowing down the degradation of admicelled rubber at 194 to 378.7°C. These indicated that the admicelled rubbers were more thermostable than natural rubber. This suggested that admicellar polymerization via the electrochemical method was a unique method to prepare a good miscible core-shell structure of PTh-NR. The mechanical properties from tensile testing showed the decrease of work to break of the admicelled rubbers. This indicated the higher stiffness of the admicelled rubbers compared to natural rubber. Since the PTh behaved like a hard and brittle material, the stiffness of the materials increased as PTh content increased. The effect of conductivity revealed that the addition of polythiophene at the same condition, 9V, 25°C, pH ~3, allowed more adsorption and adsolubilization, leading to an homogeneous coating of PTh over the rubber surface. However, too much voltage is not good to stabilize leading to the contamination in admicellar rubber due to copper corrosion. The conductivity increased from $\sigma = 10^{-15}$ S/cm at 0%wt of PTh(NR) to $\sigma = 2.61 \times 10^{-6}$ S/cm at 65%wt PTh (800mM). As PTh content increased, the conductivity was also increased because the coating of PTh was more perfect at higher concentration, as supported by TEM and SEM micrographs and the result of TGA. The higher number of polymer chains was obtained when content was high to abstract electron from thiophene and enhance free radical polymerization, resulting in higher conductivity and greater in their density.

5.6 Acknowledgements

The authors would like to acknowledge the Rachadapisek Sompoch Endevelopment (RU), Chulalongkorn University, for their financial support for this project. The author would like to acknowledge the Petroleum and Petrochemical College; the National Excellence Center for Petroleum, Petrochemicals, and Advanced Materials, Thailand; the National Research Council of Thailand.